DOCTORAL DISSERTATION

Novel Bis(spiroacridan)-substituted Dihydrophenanthrene Derivatives: Structural Features and Development toward Memory Units Based on Dynamic Redox Properties

（新規なビス（スピロアクリダン）置換ジヒドロフェナントレン誘導体: 構造的特徴と動的酸化還元挙動に基づくメモリーユニットへの展開）

Kazuhisa Wada
Graduate School of Chemical Sciences and Engineering
Hokkaido University
2013

Contents

Chapter 3

Construction of 9,9,10,10-tetraaryldihydrophenanthrene-type Dynamic Redox Systems working on Au surface

General introduction

0-1 9,9,10,10-tetraaryldihydrophenanthrene derivatives as response systems and their structural features

9,9,10,10-Tetraaryldihydrophenanthrenes (DHPs)[1] is known to be one of the most special organic redox systems. DHPs and the corresponding biphenylic dications are interconverted by redox reactions accompanied by C^9-C^{10} bond creavage/formation (Scheme 0-4). In these systems, drastic color change occurs upon redox reaction, so that this system can act as electrochromic systems. In addition, these systems show high electrochemical bistability because of their large structural changes upon redox reactions. This feature gives big advantages as response systems: large separation of redox potentials prevents the electron exchange between DHP and dication, thus exchange of oxidation state is suppressed even if DHP and dication coexist. This behavior plays important roles to realize redox-based memory units described below.

Furthermore, steric repulsion between two bulky Ar_2C moieties gives some special structural features of DHPs. As one of the examples, DHPs have a long C-C bond between C^9 and C^{10} atoms [longer than 1.6 Å][2]. Another feature is the helical structure of dihydrophenanthrene skeleton, thus DHPs have asymmetric element of helicity[3]. In this thesis, these features are revisited to explore novel aspect of DHPs. The author especially focus on the spiro bis(10-methylacridan) derivatives.

Scheme 0-4

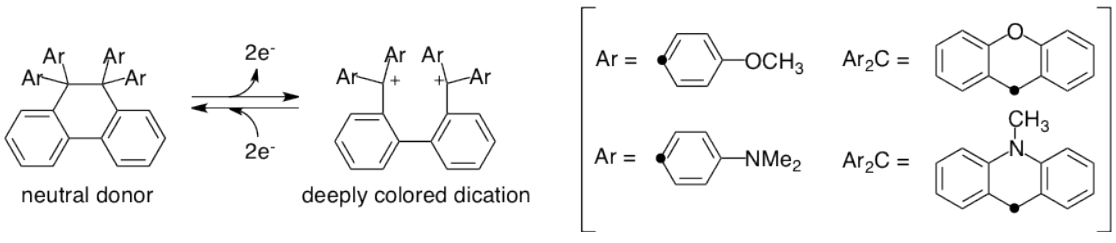

0-2 Expansion of C-C bond

Since early times, expansion of C-C single bond (standard value is 1.54 Å) have been tried by many groups[4]. The C-C bond expansion and construction of ultralong C-C bond is fundamentally important for bringing out the nature of C-C covalent bond. One of the methods to expand C-C bond is utilization of steric repulsion. From this viewpoint, hexaphenylethane skeleton is an effective motif because of large steric repulsion among six benzene rings. For example, Mislow[4b] reported the expanded C-C bond of hexakis(3,5-di-*tert*-butyl)ethane (Figure 0-1), whose central C-C bond was determined to be 1.67(3) Å.

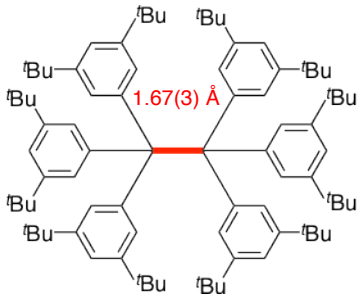

Figure 0-1. Hexaphenylethane derivatives reported by Mislow

One of the intriguing characteristics in the very long C-C bond is the "expandability" found in tetraarylpyracene derivatives which were reported in the author's laboratory by Takeda[5] and Uchimura[6]. They have introduced various aryl groups on the C^1 and C^2 position and investigated the substituent effects on the C-C bond length. According to their results, planarity of pyracene skeleton, in other words, front strain between diarylmethane moieties is the main factor that causes C-C bond expansion, although the electronic effect of aryl groups into pyracene skeleton is still not clear.

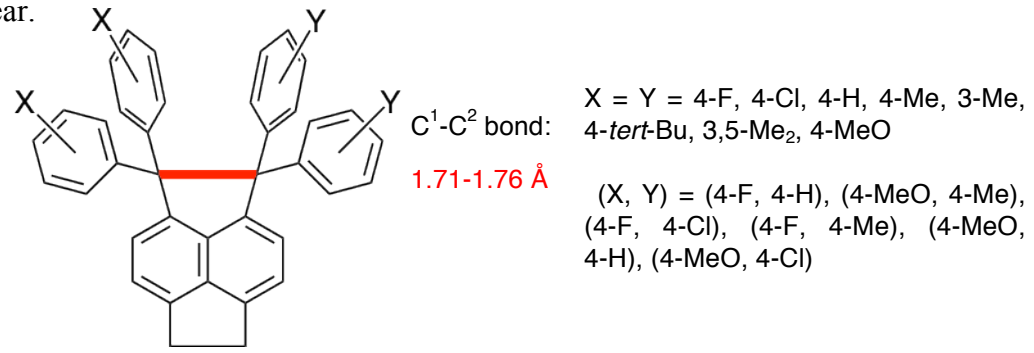

Figure 0-2. Tetraarylpyracene reported in the author's laboratory

0-3 Molecular-based switching systems and data storage devices

Recently, molecular switches, whose two different states can be interconverted by external stimuli, have been studied in many research groups[7]. One of the purposes of these researches is construction of the novel data storage devices in order to break through the limit of the memory storage density in present silicon-based devices.

As one of the examples, Irie has developed the diarylethene-type photochromic systems.[7a] These molecules can take two different state: one is the open-ring form (**A**) and the other is the closed-ring form (**B**), which each state of A and B show different colors (Scheme 0-1). Interconversion of **A** and **B** can be accomplished by irradiation of visible and UV light. Due to this response feature, diarylethenes are promising candidates for molecular-based data storage devices.

Scheme 0-1

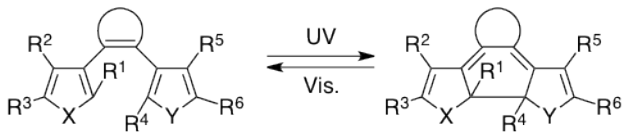

In 2002, his group reported the novel diarylethene which can response to the light in increments of few molecules,[8] which each molecule can act as 1 bit memory unit. In this system, closed-ring form (**D**) shows fluorescence while open-ring form (**C**) does not (Scheme 0-2). His group utilize this features to observe the state (closed-ring or open-ring form) of each molecule. Thus, the state of a certain molecule (open-ring or closed-ring form) are detected by observation of unimolecular fluorescence. As shown in Figure 0-3, fluorecsence of each molecule was succesfully observed.

Scheme 0-2

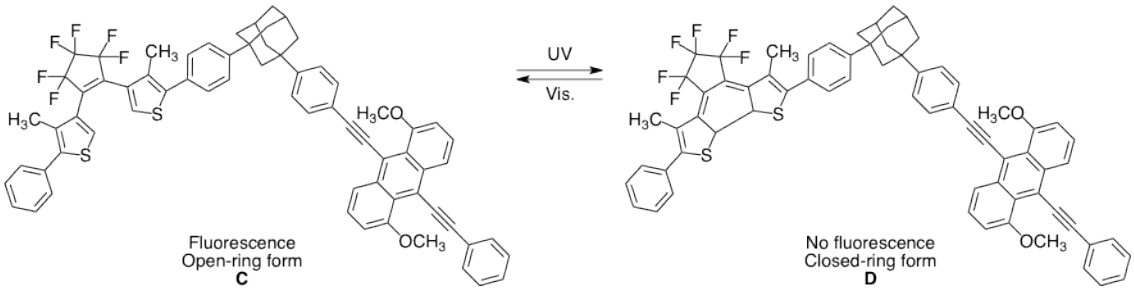

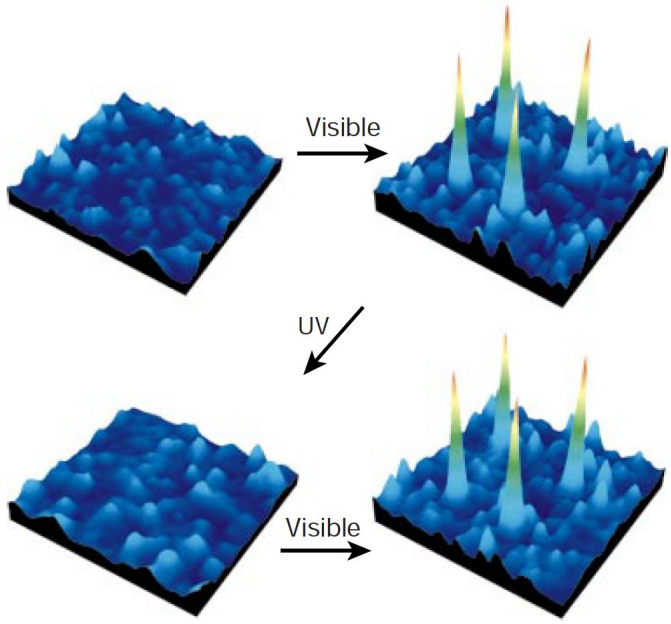

Figure 0-3. Fluorescence images of single photoswitching molecules of the open- and closed-ring of a compound.

As another example of unimolecular response systems, Yamashita[9] reported the double-decker bis(phthalocyaninato)terbium(III) complex. In this complex, rotation of phthalocyanin ligand and appearance and disappearance of Kondo peak are induced by conducting the current. Interconversion of two states were successfully observed in STM images (Figure 0-4).

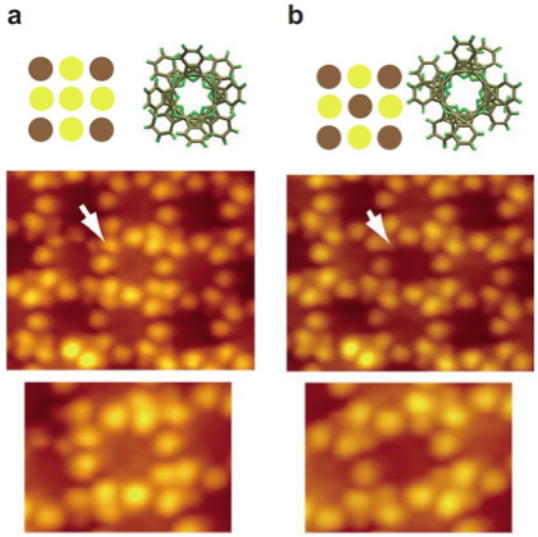

Figure 0-4. Molecular manipulation and control of Kondo feature.

0-4 Transmitting and memorizing the chirality as information

The intermolecular transmission of asymmetric information is one of the most important events in natural biological systems as well as in the field of supramolecular chemistry.[10] Chiral-memory units play important roles in the above phenomenon, where they act as asymmetric-information receptors and store chiral information transmitted from the sourse. Heretofore, a variety of chiral memories have been reported.[11] As one of the examples, Yashima and his coworkers[12] reported the polymers with a function of chiral memory. In this polymer **E**, macromolecular helicity was induced by adding (*R*)-1-naphthylethylamine (*R*)-**F** (left-handed helix) or (*S*)-2-methyl-1-propanol (*S*)-**G** (right-handed helix), and the resulting induced helix can be converted into non-helical structure upon addition of CF_3CO_2H (Scheme 0-3). In this system, non-helical and helical state can be regarded as ”erasable/writable state” and memorizing state” of chiral information, respectively. Many studies have been carried out by using helical polymers, and studies on non-polymeric materials are rare.

Scheme 0-3

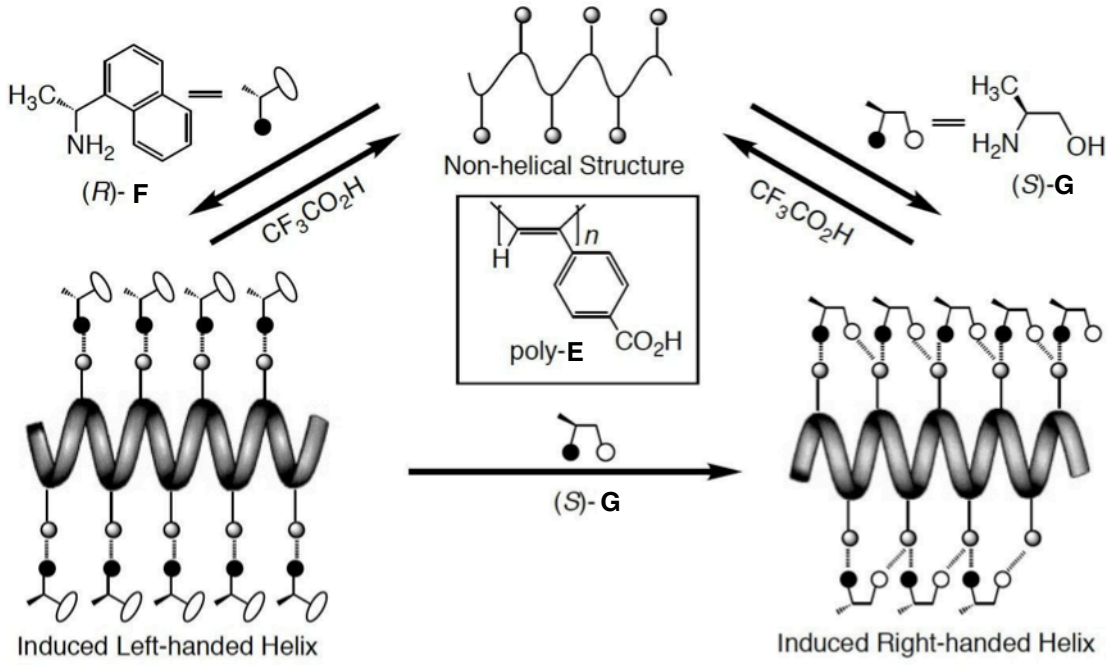

0-5 Summary of the thesis

In Chapter 1, novel steric effect of the DHP is described by featuring bis(10-methylspiroacridan)derivative. Thus, steric repulsion at the remote positions affects the C^9-C^{10} bond through biphenyl skeleton (Figure 0-5). Systematic analyses of newly prepared DHP derivatives with various substituents at C^4, C^5 position by X-ray, it was found that bulkiness of substituents at the bay region and C^9-C^{10} bond length showed a positive correlation. This result can be accounted for by considering that steric bulkiness of substituents in the bay region induce the twisting of biphenyl skeleton to lead the C^9-C^{10} expansion.

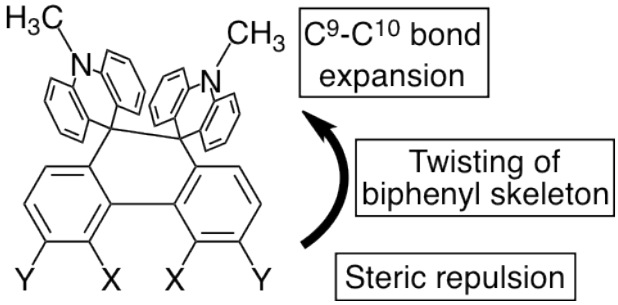

Figure 0-5.

In Chapter 2, the novel redox-based chiral memory by using DHP skeleton is described. By introducing proper bridging unit into DHP skeleton, control of steric inversion by redox reaction was successfully accomplished. Thus, easy ring flip occurs in neutral state, whereas ring flip was suppressed in the dicationic state. In this system, asymmetric information is stored in dicationic state and erased in neutral state (Scheme 0-5).

Scheme 0-5

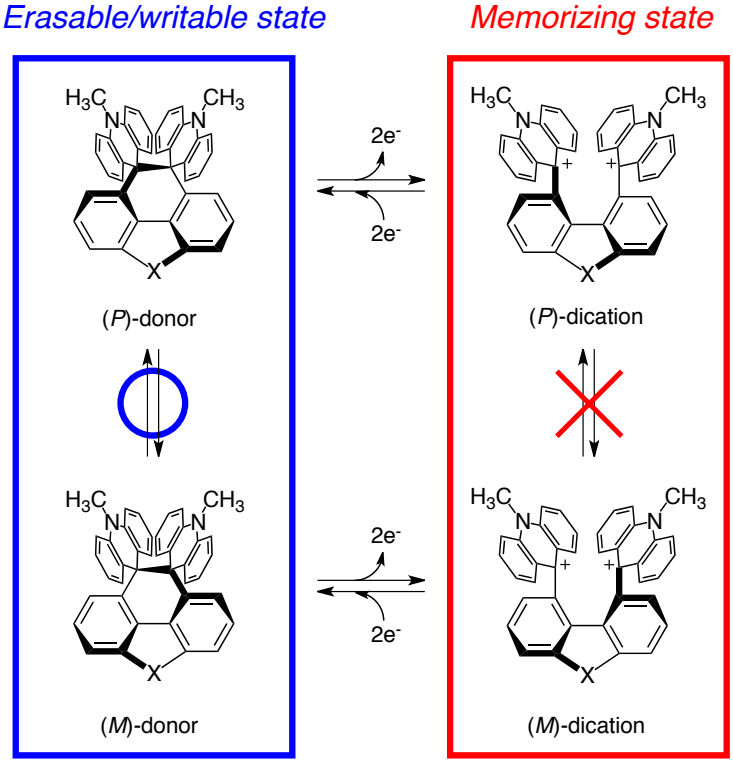

In Chapter 3, the author has investigated the DHP type redox systems which can work on Au electrode toward the realization of advanced memory unit (Scheme 0-6). DHP derivatives with lipoic and isolipoic ester as anchoring group toward Au surface were prepared and their immobilization on Au(111) atoms was investigated. Observed redox species were identified by surface IR spectroscopy. On the Au(111) electrode, electrochemical bistability was found to decrease compared with CH_2Cl_2 state.

Scheme 0-6

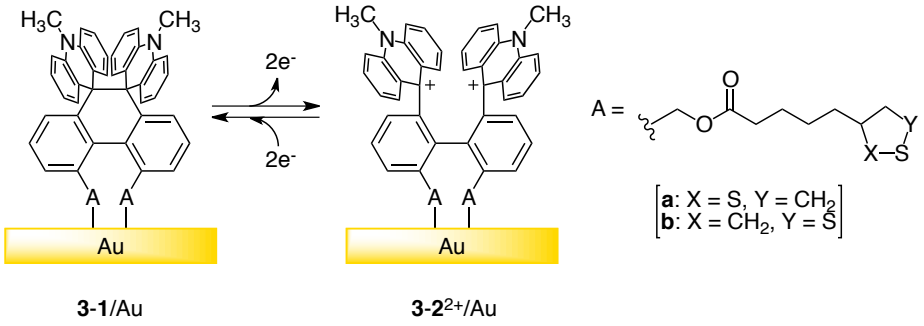

References

[1] T. Suzuki, E. Ohta, H. Kawai, K. Fujiwara, T. Fukushima, *Synlett* **2007**, 851.

[2] a) T. Suzuki, K. Ono, J. Nishida, H. Takahashi, T. Tsuji, *J. Org. Chem.* **2000**, *65*, 4944.; b) T. Suzuki, A. Migita, H. Higuchi, H. Kawai, K. Fujiwara, T. Tsuji, *Tetrahedron Lett.* **2003**, *44*, 6837.

[3] a) J. Nishida, T. Suzuki, M. Ohkita, T. Tsuji, *Angew. Chem. Int. Ed.* **2001**, *40*, 3251.; b) T. Suzuki, R. Yamamoto, H. Higuchi, E. Hirota, M. Ohkita, T. Tsuji, *J. Chem. Soc. Perkin Trans. 2* **2002**, 1937.: c) T. Suzuki, Y. Ishigaki, T. Iwai, H. Kawai, K. Fujiwara, H. Ikeda, Y. Kano, K. Mizuno, *Chem. Eur. J.* **2009**, *131*, 16896.

[4] a) D. A. Dougherty, W. D. Hounshell, H. N. Schlegel, R. A. Bell, K. Mislow, *Tetrahedron Lett.* 1976, 39, 3479.; b) B. Kahr, D. Van Engen, K. Mislow, *J. Am. Chem. Soc.* **1986**, *108*, 8305.; b) E.Osawa, P. M. Ivanov, C. Jaime, *J. Org. Chem.* **1983**, *48*, 3990.; c) K. Tanaka, N. Takamoto, Y. Tezuka, M. Kato, F. Toda, *Tetrahedron* **2001**, *57*, 3761.; d) H. Kawai, T. Takeda, K. Fujiwara, T. Inabe, T. Suzuki, *Cryst. Growth Des*. **2005**, *5*, 2256.

[5] T. Takeda, H. Kawai, R. Herges, E. Mucke, Y. Sawai, K. Murakoshi, K. Fujiwara, T. Suzuki, *Tetrahedron Lett.* **2009**, *50*, 3693.

[6] T. Suzuki, Y. Uchimura, Y. Ishigaki, T. Takeda, R. Katoono, H. Kawai, K. Fujiwara, A. Nagaki, and J. Yoshida, *Chem. Lett.* **2012**, *41*, 541.

[7] a) M. Irie, *Chem. Rev.* **2000**, *100*, 1685. b) K. Matsuda, M. Irie, *J. Photochem. Photobiol. C.* **2004**, *5*, 169.; B. L. Feringa, Molecular switches, Wiley-VCH, Weinheim, 2002.; c) G. H. Brown, *Photochromism*, Wiley-Interscience, New York, **1971**; d) H. Duerr, H. Bouas-Laurent, *Photochromism: Molecules and Systems*, Elsevier, Amsterdam, **2003**.

[8] M. Irie, T. Fukaminato, T. Sasaki, N. Tamai, T. Kawai, *Nature* **2002**, *420*, 759.

[9] T. Komeda, H. Isshiki, J. Liu, Y.-F. Zhang, N. Lorente, K. Katoh, B. K. Breedlove, M. Yamashita, *Nature commun.* **2011**, *2*, 217.

[10] a) A. R. A. Palmas, E. W. Meijer, *Angew. Chem. Int. Ed.* **2007**, *46*, 8948.; b) G. A. Hembury, V. V. Borovkov, Y. Inoue, *Chem. Rev.* **2008**, *108*, 1.

[11] a) T. Ishi-i, M. Crego-Calama, P. Timmerman, D. R. Reinhoudt, S. Shinkai, *J. Am. Chem. Soc.* **2002**, 124, 14631.; b) R. D. Rasberry, X. Wu, B. N. Bullock, M. D. Smith, K. D. Shimizu, *Org. Lett.* **2009**, *11*, 2599.; c) M. Ishikawa, K. Maeda, Y.

Mitsutsuji, E. Yashima, *J. Am. Chem. Soc.* **2004**, *126*, 732.; d) Y. Mizuno, T. Aida, K. Yamaguchi, *J. Am. Chem. Soc.* **2000**, *122*, 5278.; e) R. Randazzo, A. Mammana, A. D'Urso, R. Lauceri, R. Purrello, *Angew. Chem. Int. Ed.* **2008**, *47*, 9879.; **2009**, *48*, 1351.

[12] E. Yashima, K. Maeda, Y. Okamoto, *Nature* **1999**, *399*, 449.

Chapter 1

Transmission of Steric Effect into Remote Position: C^9-C^{10} bond expansion of 9,9,10,10-tetraaryldihydrophenanthrene skeleton induced by substituents in the bay region

1-1 Introduction

In the author's laboratory, various derivatives of the 9,9,10,10-tetraaryldihydrophenanthrene (DHP) have been prepared[1]. One of the interesting features of these derivatives is the long single bond between C^9 and C^{10} atoms [longer than 1.6 Å]. According to the X-ray analyses of these compounds (Figure 1-1)[1e], the DHP skeleton adopts a helical structure in order to reduce the steric repulsion between bulky diarylmethane moieties. By considering the helical structure and long C-C bond in DHPs, the author obtained the idea that an increase in torsion angle of the DHP skeleton would "pull", if possibly, the C^9-C^{10} bond to extend this bond. In order to twist the DHP skeleton further, increase of steric repulsion at the bay region would be effective by introducing bulky substituents. According to this hypothesis, the author designed several 4,5-disubstituted DHPs **1-1b-e** and dibenzo derivative **1-1f**. Spiroacridan units on C^9/C^{10} position were selected because of easiness of preparation.

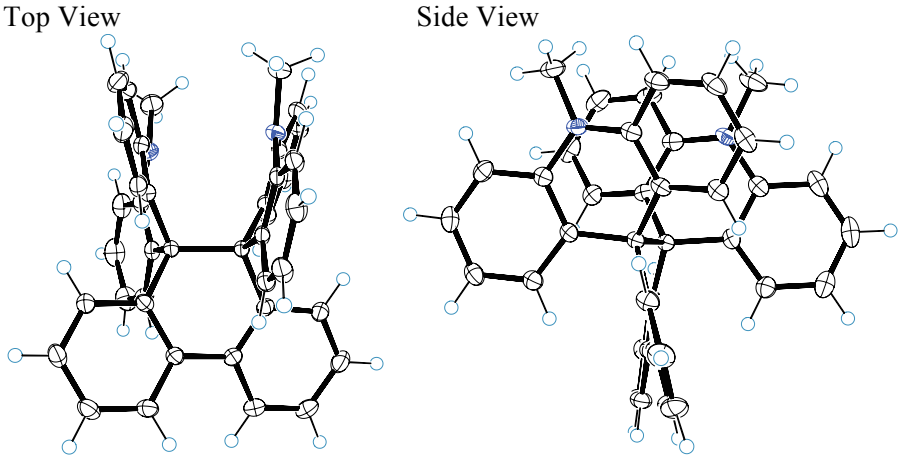

Figure 1-1. X-ray structure of bis(spiroacridan)-substituted DHP **1-1a**

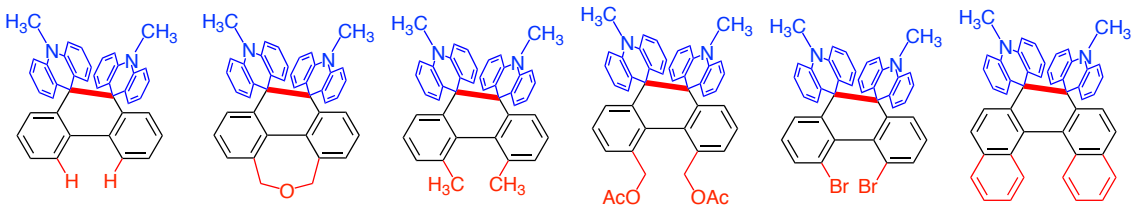

1-2 Preparation

Preparation of **1-1b**,**c**,**e**,**f** was carried out in a similar manner to **1-1a** (Scheme 1-1). Thus, dilithiobiphenyl derived from dibromides **1-3b** was reacted with 10-(2-methoxyethoxymethyl)acridone (MEM-acridone) followed by deprotection of MEM group under acidic hydrolytic conditions to gave diacridines **1-4b** in 48% yield. Double *N*-methylation of diacridine **1-4b** by CH_3OTf gave the corresponding dication salt **1-2b**$^{2+}(TfO^-)_2$ in 84% yield, which was converted to desired DHP **1-1b** upon reduction with Zn dust in 79% yield. DHPs **1-1c**,**e**,**f** were also prepared in a similar fashion except using 2,6-di(*tert*-butyl)-4-methylpyridine (DTBMP) in the *N*-methylation of **1-4c**,**e**[2],**f** and direct conversion of crude dication salt **1-2c**,**e**,**f**$^{2+}(TfO^-)_2$ into DHPs **1-1c**,**e**,**f** (y. 31%, 12% and 54%, respectively, over two steps).

Scheme 1-1

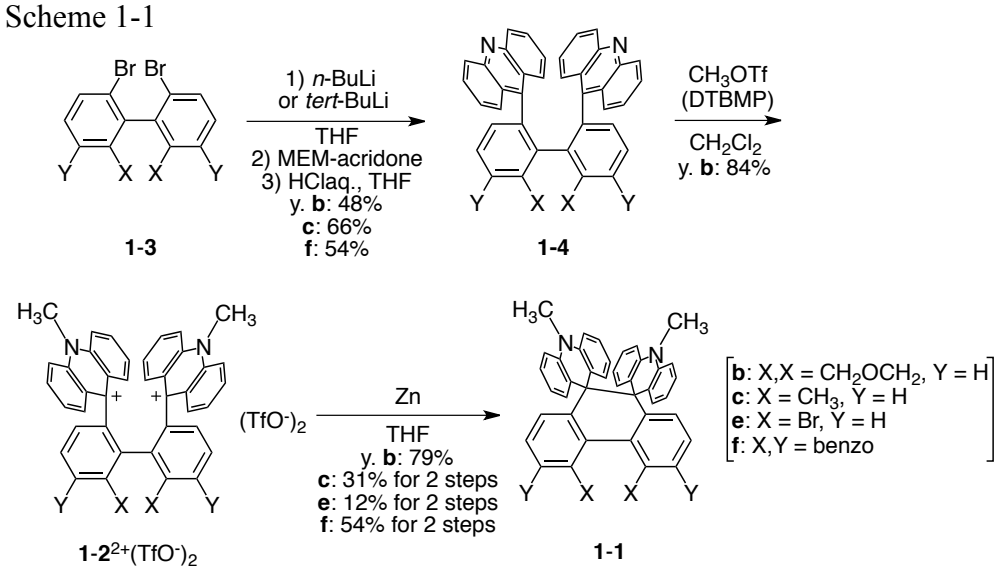

Diacetate **1-1d** was prepared as shown in Scheme 1-2. Double quaternization of diformylated diacridine **1-4g**[1k] followed by 2e-reduction gave DHP **1-1g**, whose formyl groups were directly reduced by $LiAlH_4$ to give diol **1-5** in 61% over 3 steps. Acetylation of this diol gave DHP **1-1d** in 63% yield.

Scheme 1-2

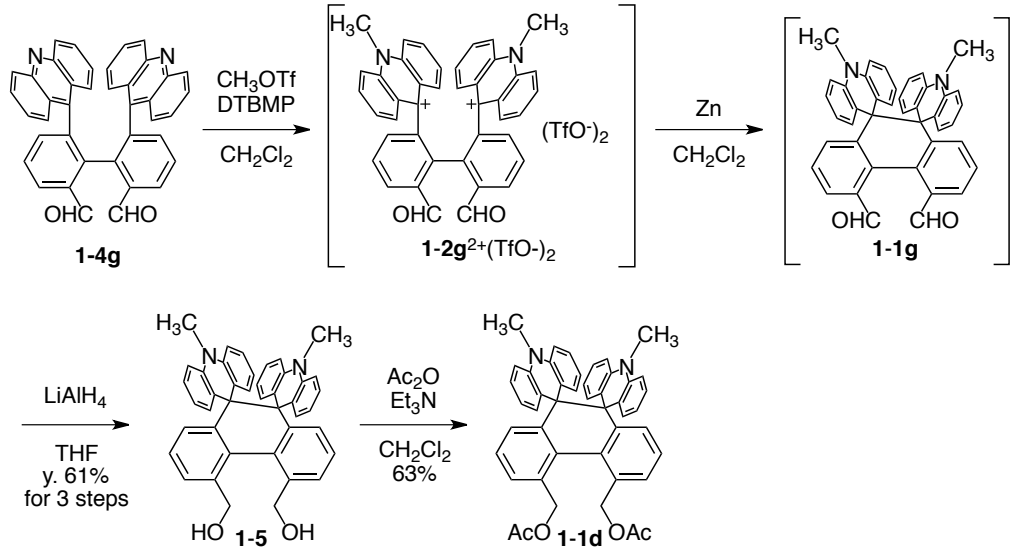

1-3 X-ray analyses

1-3-1 X-ray structures of 1-1a-f

Newly obtained DHPs **1-1b-f** were recrystallized by a vapor diffusion method ($C_6H_6/CH_2Cl_2/CHCl_3$-hexane) to give single crystalline samples, and their X-ray stractural analyses were conducted at -123 ˚C. The molecular structures are shown in Figures 1-2 - 1-6. There are no structural disorders although the crystals of **1-1b**, **1-1c** and **1-1e** were obtained as solvates. In these structures, DHP molecules have a long C^9-C^{10} bond and adopt a helical structure, as expected. It is evident that the newly prepared DHPs suffer from two major steric hindrances: one is the strain between the two butterfly-shaped spiroacridan units over the C^9-C^{10} bond, and the other is repulsion between the C^4/C^5-substituents or between fused benzene rings in the bay region. X-ray structures in hands, structural comparisons were carried out with those of previously reported molecules **1-1a** and *N*-propargyl derivatives **1-1a'**[1i].

Top View

Side View

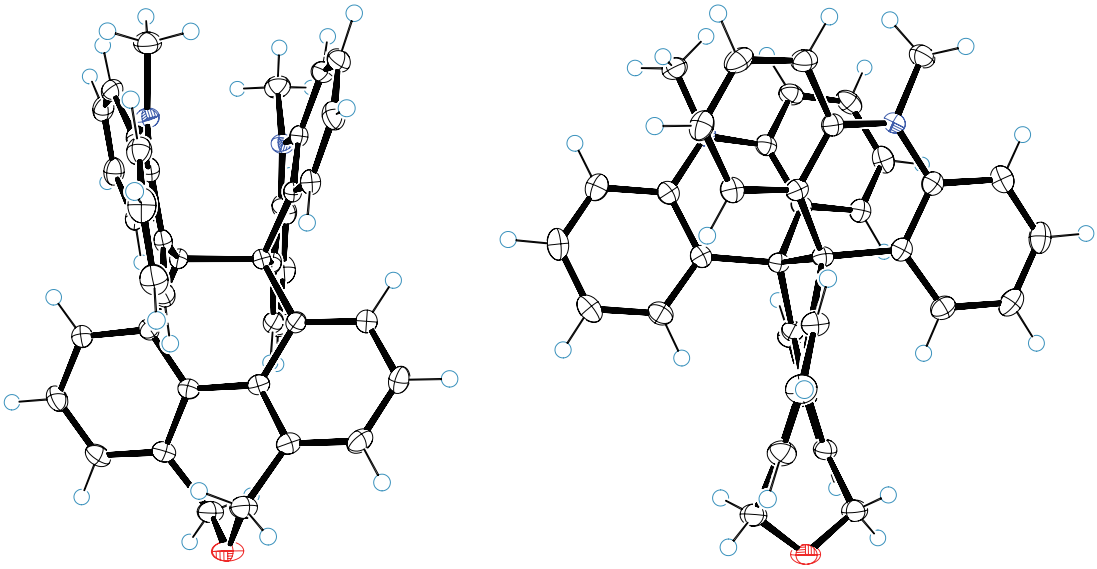

Figure 1-2. X-ray structure of **1-1b** in **1-1b**•C_6H_6 crystal

Top View

Side View

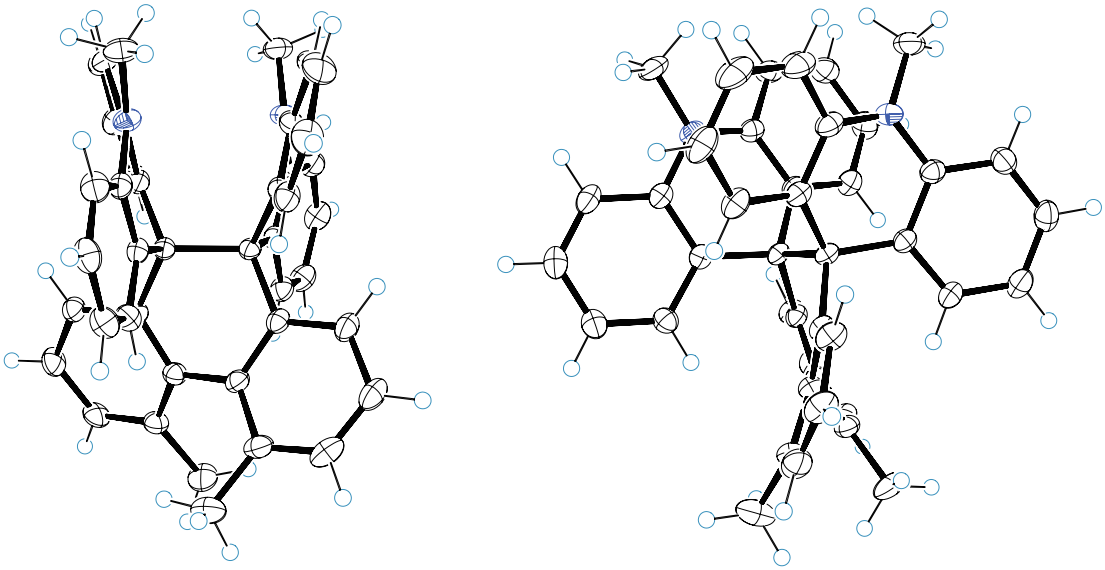

Figure 1-3. X-ray structure of **1-1c** in **1-1c**•$CHCl_3$ crystal

Top View

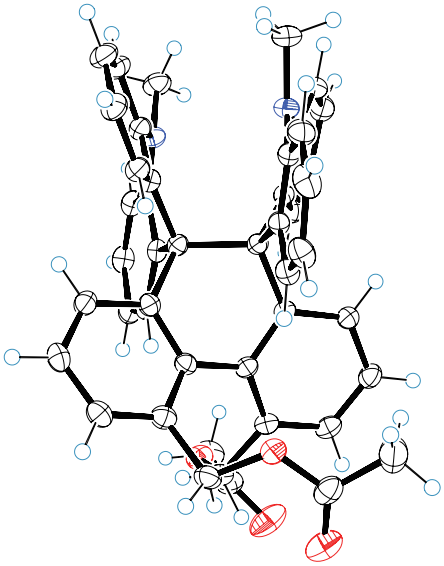

Side View

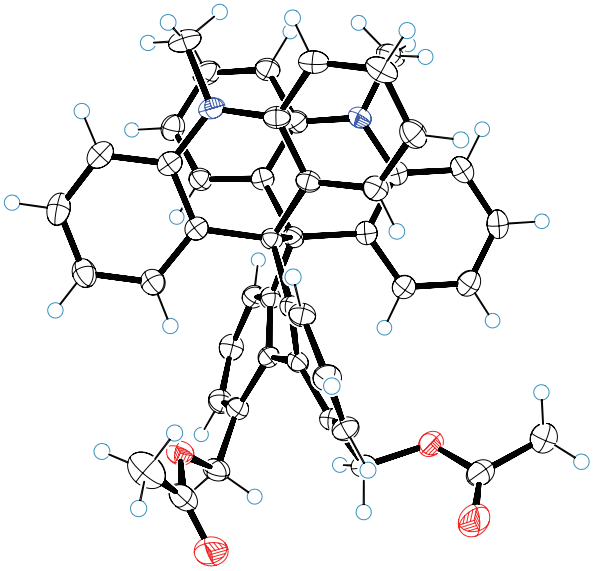

Figure 1-5. X-ray structure of **1-1d** in **1-1e**•$2CH_2Cl_2$ crystal

Top View

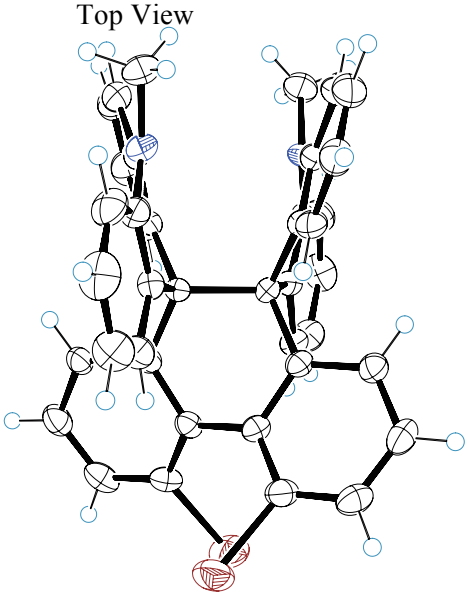

Side View

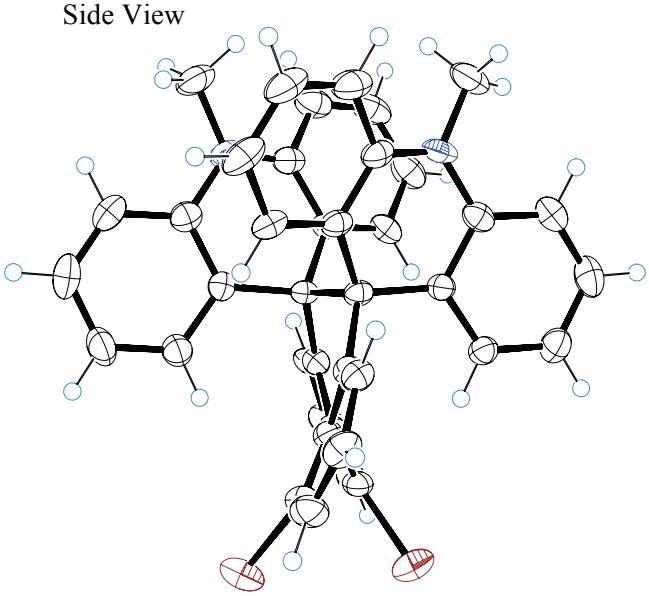

Figure 1-4. X-ray structure of **1-1e**

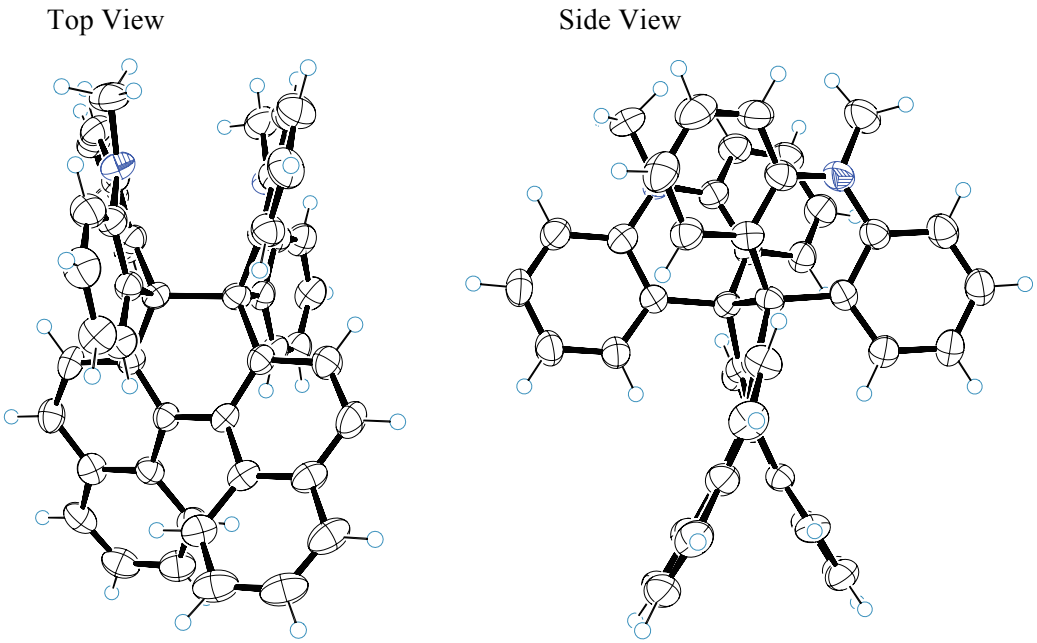

Figure 1-6. X-ray structure of **1-1f**

1-3-2 Torsion of skeleton and C-C bond lengths

The structural parameters are summarized in Tables 1-1 and 1-2. the C^4--C^5 distance (*D*) is much greater in **1-1c-f** [3.126(2)-3.179(7) Å] than that in **1-1a** [1.634(2) Å]. More importantly, all of the C^9-C^{10} bond length (*d*) in **1-1c-f** [1.649(3)-1.652(6) Å] are significantly greater than that in **1-1a** [1.634(2) Å] despite the fact that the substituents at the C^4/C^5 positions or fused benzene rings never increase the steric factors around the C^9-C^{10} bond directly. There is an essentially monotonic relationship between *d* and *D* (Figure 1-7), showing that the observed expansion of the C^9-C^{10} bond is not related to the crystallographic artifacts but surely come with geometrical remote steric effects.

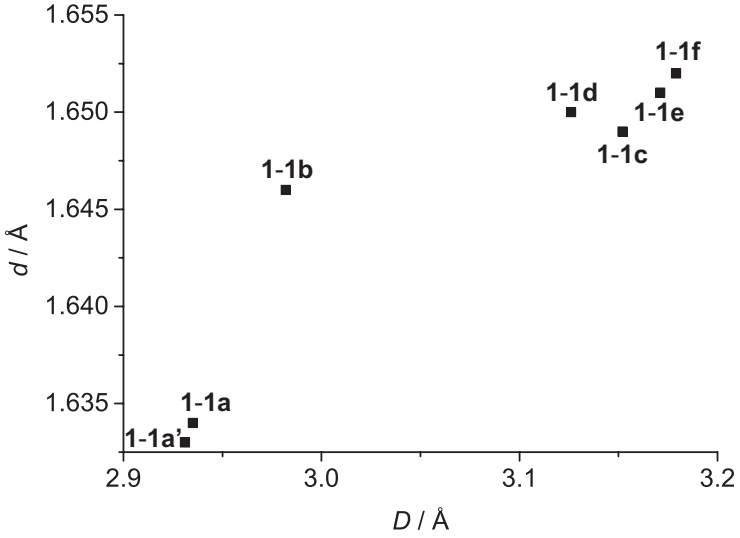

Figure 1-7. Scattering plot of C^4-- C^5 distance (*D*) *vs.* C^9-C^{10} bond length (*d*) determined by low-temperature X-ray analyses

Table 1-1. Crysltal parameters of DHPs **1-1a-f** determined by low-temperature X-ray analyses

	1-1a	**1-1a'**•$5C_6H_6$	**1-1b**•C_6H_6	**1-1c**•$CHCl_3$	**1-1d**	**1-1e**•$2CH_2Cl_2$	**1-1f**
space group	$P2_1/n$	$Pccn$	$C2/c$	P-1	$P2_1/n$	$P2/c$	P-1
a / Å	13.094(3)	11.899(1)	23.560(4)	9.539(2)	12.847(3)	19.235(4)	9.668(9)
b / Å	13.376(3)	17.125(2)	11.900(2)	10.253(2)	14.904(3)	12.036(2)	10.494(9)
c / Å	15.540(4)	29.198(3)	13.927(2)	19.077(4)	17.656(4)	14.145(3)	17.86(2)
α / °				94.613(3)			97.323(13)
β / °	92.231(3)		120.2315(5)	90.4991(10)	100.818(2)	95.459(2)	92.235(6)
γ / °				117.523(4)			114.47(2)
V / Å^3	2719(1)	5949.5(9)	3373.5(9)	1647.0(6)	3320.6(10)	3259.8(9)	1627(3)
Z	4	4	4	2	4	4	2
R / %	4.61	7.62	4.68	9.96	5.62	8.63	12.04

Table 1-2. Structural parameters of DHPs **1-1a-f** determined by low-temperature X-ray analyses

	1-1a	**1-1a'**• $5C_6H_6$	**1-1b**• C_6H_6	**1-1c**• $CHCl_3$	**1-1d**	**1-1e**• $2CH_2Cl_2$	**1-1f**
C_9-C_{10} bond length (d) / Å	1.634(2)	1.633(2)	1.646(2)	1.649(3)	1.650(2)	1.651(6)	1.652(6)
Torsion angle (φ_1) / °	17.5(2)	17.7(3)	30.7(2)	41.1(4)	39.0(2)	40.6(7)	42.7(6)
Torsion angle (φ_2) / °	19.5(2)	19.1(3)	26.7(2)	34.8(4)	35.6(2)	34.7(6)	32.2(6)
Torsion angle (φ_3) / °	47.1(1)	45.3(2)	48.9(1)	51.0(3)	48.5(1)	50.5(4)	50.4(5)
C_4-C_5 distance (D) / Å	2.935(2)	2.931(2)	2.982(2)	3.152(4)	3.126(2)	3.171(7)	3.179(7)

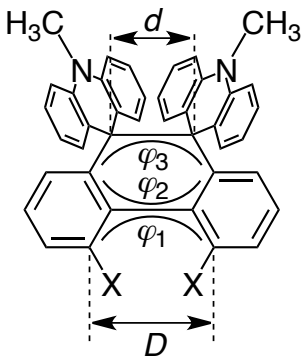

Further discussion of this geometric remote steric effect was carried out by

considering the torional parameters of DHP skeleton. Three torsion angles defined by C^4-C^{4a}-C^{5a}-C^5 (φ_1), C^{10a}-C^{4a}-C^{5a}-C^{8a} (φ_2), and C^{8a}-C^9-C^{10}-C^{10a} (φ_3) was found to be larger than that in **1-1a**. As shown in Figures 1-8 - 1-10, these three torsions also have monotonic relationship with C^9-C^{10} bond length (*d*), showing twisting deformation of the DHP skeleton is the key to transfer the steric bulkiness from the C^4/C^5 position to the C^9-C^{10} bond to cause additional strain and realize geometrical remote steric effects in **1-1c-f**.

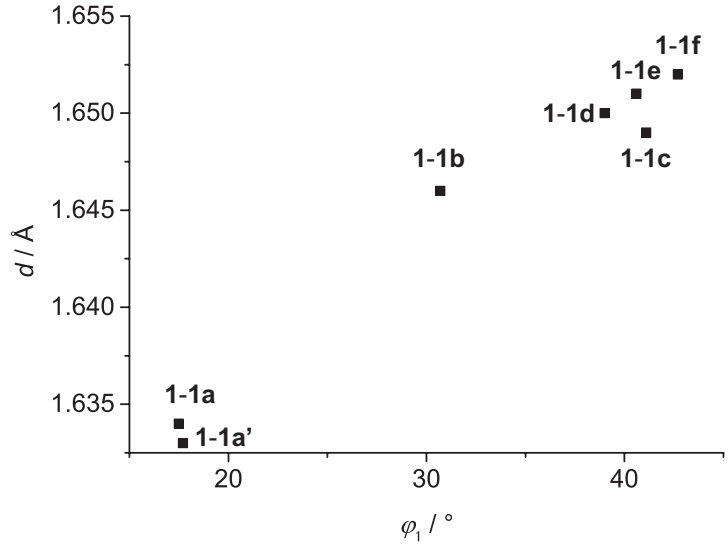

Figure 1-8. Scattering plot of torsion angle in C^4-C^{4a}-C^{5a}-C^5 (φ_1) *vs.* C^9-C^{10} bond (*d*) determined by low-temperature X-ray analyses

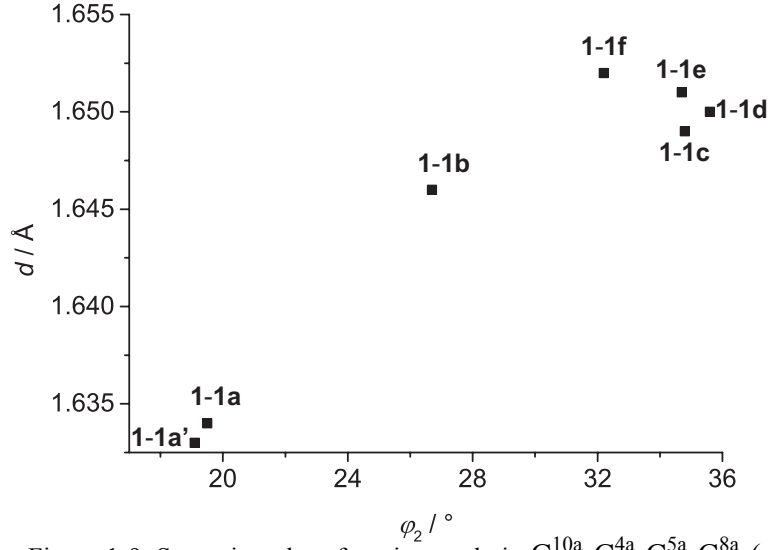

Figure 1-9. Scattering plot of torsion angle in C^{10a}-C^{4a}-C^{5a}-C^{8a} (φ_2) *vs.* C^9-C^{10} bond (*d*) determined by low-temperature X-ray analyses

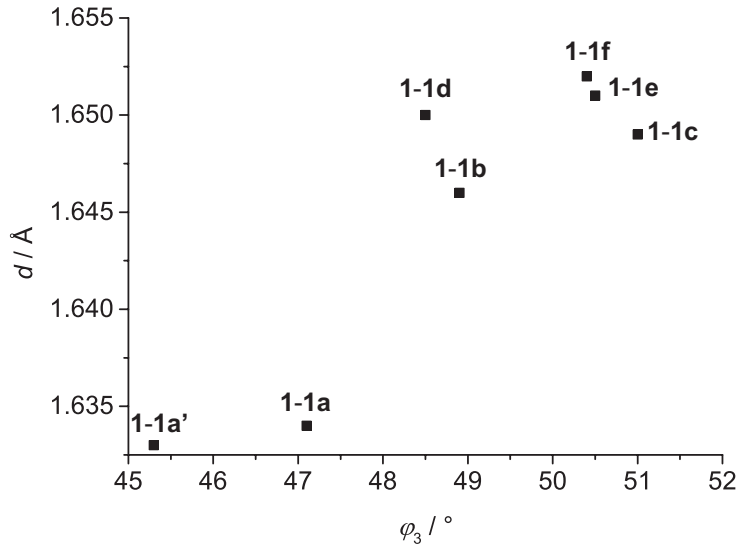

Figure 1-10. Scattering plot of torsion angle in C^{8a}-C^{9}-C^{10}-C^{10a} (φ_3) *vs.* C^{9}-C^{10} bond (*d*) determined by low-temperature X-ray analyses

Finally, the observed steric effects were compared with the results about 9,10-unsubstituted dihydrophenanthrene derivatives reported by Sternhell[3]. In the 9,10-unsubstituted derivatives, such steric effects are not present. Thus in the scattering plot of the C^{9}-C^{10} bond length (*d*) versus C^{4}--C^{5} distance (*D*) as in the case of **1-1**, no meaningful correlation was found (Figure 1-11). This difference is in line with the nature of prestrained bonds predicted by Osawa[4], thus the prestrained bonds are more susceptible to structure of perturbation in terms of bond elongation.

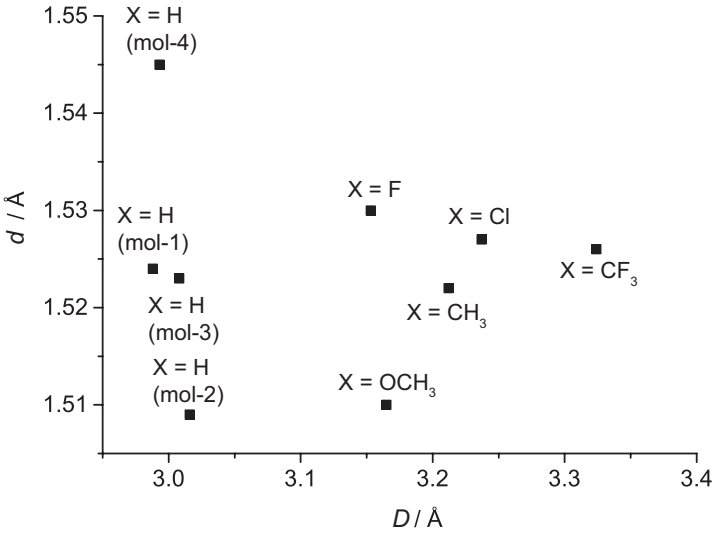

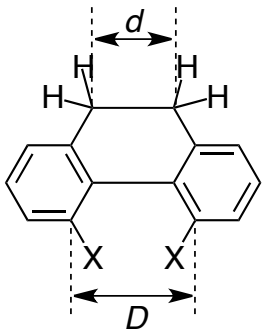

Figure 1-11. Scattering plot of C^{4}-- C^{5} distance (*D*) *vs.* C^{9}-C^{10} bond length (*d*) reported by Sternhell

1-4 Summary

In this chapter, the author prepared the some DHP compounds **1-1b-f** with various substituents in C^4 and C^5 position, and X-ray analyses of these compounds were conducted. According to the structural parameters determined by X-ray analyses, C^9-C^{10} bond length (*d*) shows positive correlation with torsional parameters (*D*, φ_1-φ_3) of DHP skeleton. From these results, existence of geometrical remote steric effect, which steric repulsion of substituents in C^4 and C^5 position induces C^9-C^{10} bond expansion via torsional escalation of biphenyl moiety, was suggested.

Experimental section

General

^{1}H and ^{13}C NMR spectra were recorded on a JEOL AL-300 (^{1}H 300 MHz and ^{13}C 75 MHz) and α400 (^{13}C 100 MHz) spectrometer. Chemical shifts (δ) were reported with TMS (in $CDCl_3$, δ=0.00 ppm) or CH_3CN (in CD_3CN, δ=1.93 ppm) as internal standards. IR spectra in KBr tablet dice were recorded on a JEOL WINSPEC100 infrared spectrophotometer. Mass spectra were recorded on a JEOL JMS-600H in EI mode, and on a JMS-AX500 spectrometers in FD mode (GC-MS & NMR Laboratory, Graduate School of Agriculture, Hokkaido University). Elemental Analyses were taken on J-Science micro corder JM10 or on a Yanaco CHN corder MT-6 at the Instrumental Analysis Division, Equipment Management Center, Creative Research Institution, Hokkaido University. Cyclic voltammograms in CH_2Cl_2 were measured with a BAS ALS-600A electrochemical analyzer. X-ray diffraction data for single-crystal analysis were measured by a RIGAKU AFC-5R + Mercury CCD apparatus (50 kV, 200 mA). Flash chromatography was performed on silica gel I-6-40 (YMC) of particle size 40-63 μm and on aluminum oxide 90 standardized (Merck 63-200 μm). Melting points were measured on a Yamato MP-21 and reported uncorrected. UV-Vis spectra were recorded on a Hitachi U-3500 spectrophotometer. Fluorescence spectra were measured on a Hitachi F-4500 spectrofluorometer. All commercially available compounds and solvents were used without further purification except for THF (distilled from Na by using benzophenone as an indicator, or purified by Nikko Hansen GlassContour Solvent Dispensing System) and CH_3CN (distilled from CaH_2 and P_4O_{10}).

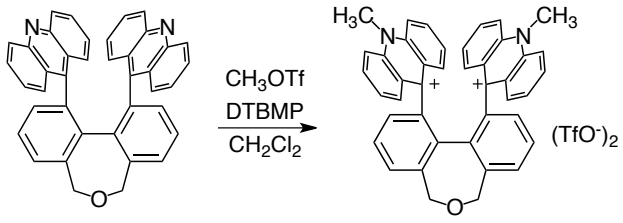

1-4b **1-2b**$^{2+}$ $(TfO^-)_2$

Preparation of 5,7-dihydrodibenz[*c*,*e*]oxepin-1,11-diylbis(10-methyl-9-acridinium) **1-2b**$^{2+}(TfO^-)_2$

To a solution of 9,9'-(5,7-dihydrodibenz[*c*,*e*]oxepin-1,11-diyl)diacridine **1-4b**[2] (158 mg, 287 μmol) in dry CH_2Cl_2 15 mL was added dropwise methyl trifluoromethanesulfonate (320 μL, 2.83 mmol) under Ar. After stirring for 17 h at 25 ˚C, the mixture was diluted with dry Et_2O. The resulting precipitates were filtered and washed with dry Et_2O, and dried in vacuo to give **2-2b**$^{2+}(TfO^-)_2$ (212 mg) as a yellow solid in 84% yield.

data for **1-2b**$^{2+}(TfO^-)_2$: m.p. 270-279 ˚C (decomp.); ^{1}H NMR (300 MHz, CD_3CN) δ 8.40 (2H, d, J = 9.4 Hz), 8.23 (2.0 Hz, dd, J = 6.4 Hz, 9.4 Hz), 8.12 (2H, ddd, J = 1.3 Hz, 6.4 Hz, 9.0 Hz), 7.97 (2H, d, J = 9.0 Hz), 7.89 (2H, dd, J = 1.3 Hz, 7.6 Hz), 7.54-7.67 (4H, m), 7.59 (2H, dd, J = 7.6 Hz, 7.6 Hz), 7.24 (2H, ddd, J = 0.9 Hz, 6.7 Hz, 8.9 Hz), 6.95 (2H, dd, J = 1.3 Hz, 7.6 Hz), 6.25 (2H, dd, J = 1.4 Hz, 8.9 Hz), 5.01 (2H, d, J = 11.8 Hz), 4.61 (2H, d, J = 11.8 Hz), 4.39 (6H, s); ^{13}C NMR (75 MHz, CD_3CN) δ 141.88, 140.94, 140.38, 139.34, 139.11, 138.65, 136.33, 134.41, 130.70, 129.84, 128.80, 128.18, 127.95, 124.17, 119.93, 119.63, 118-119, 68.19, 39.56; IR (KBr) ν cm^{-1} 3110, 2926, 2868, 1609, 1579, 1549, 1460, 1374, 1275, 1224, 1159, 1030, 862, 766, 745, 709, 637, 571, 518; LR-MS (FAB) *m*/*z* 580 (M^+, 7), 565 ($[M-CH_3]^+$, 5), 391 (11), 281 (12), 220 (15), 207 (17), 149 (96), 74 (BP); HR-MS (FAB) Calcd. for $C_{42}H_{32}N_2O$: 580.2517, Found : 580.2526; Cyclic voltammetry (in CH_3CN, 0.1 M Et_4NClO_4, 0.1 V s^{-1}): E^{red} = -0.20 V *vs.* SCE (irrev.); Cyclic voltammetry (in CH_2Cl_2, 0.1 M Bu_4NClO_4, 0.1 V s^{-1}): E^{red} = -0.43 V *vs.* Ag/Ag^+; Anal. Calcd. for $C_{44}H_{32}F_6N_2O_7S_2 \cdot H_2O$: C 58.92, H 3.82, N 3.12. Found: C 58.93, H 3.78, N 3.03.

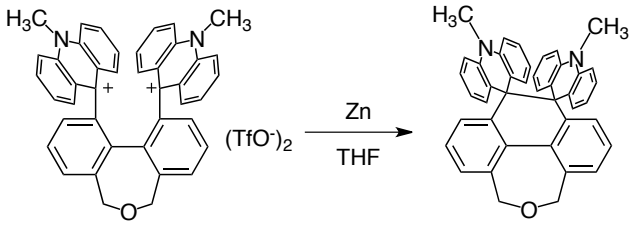

1-2b^{2+} $(TfO^-)_2$ **1-1b**

Preparation of dispiro[(10-methylacridan)-9,10'(4'*H*,6'*H*,10'*H*,11'*H*)-phenanthr[4',5'-*cde*]oxepin-11',9''-(10''-methylacridan)] **1-1b**

A suspension of **1-2b**$^{2+}(TfO^-)_2$ (51.2 mg, 58.3 μmol) and Zn powder (154 mg, 2.64 mmol) in dry THF 2.5 mL was stirred at 25 ˚C for 17 h. After diluted with water, the whole mixture was extracted with CH_2Cl_2. The combined organic layers were washed with water and brine, and dried over Na_2SO_4. After filtration, solvent was concentrated under reduced pressure. The residue was purified by flash chromatography on aluminum oxide (hexane : toluene = 10 : 1, 0.5% v/v triethylamine (Et_3N)) to give **1-1b** (26.9 mg) as a colorless powder in 79% yield.

data for **1-1b**: m.p. 292-296 ˚C (decomp.); ^{1}H NMR (300 MHz, $CDCl_3$) δ 7.45 (2H, dd, J = 1.3 Hz, 7.3 Hz), 7.22 (2H, dd, J = 7.3 Hz, 7.3 Hz), 7.11 (2H, dd, J = 1.3 Hz, 7.3 Hz), 6.98 (4H, ddd, J = 1.5 Hz, 7.0 Hz, 8.2 Hz), 6.51 (4H, d, J = 8.2 Hz), 6.33 (4H, dd, J = 7.0 Hz, 7.0 Hz), 6.13-6.39 (4H, br), 4.64 (4H, s), 2.73 (6H, s); IR (KBr) ν 3059, 2956, 2871, 2848, 1591, 1476, 1362, 1323, 1292, 1272, 1167, 1135, 1084, 1070, 1058, 901, 868, 791, 755, 697 cm^{-1}; LR-MS (FD) m/z 580 (M^+, BP), 290 (M^{2+}, 15); Cyclic voltammetry (in CH_3CN, 0.1 M Et_4NClO_4, 0.1 V s^{-1}): E^{ox} = +0.16 V *vs.* SCE (irrev.); Cyclic voltammetry (in CH_2Cl_2, 0.1 M Bu_4NClO_4, 0.1 V s^{-1}): E^{ox} = +0.04 V *vs.* Ag/Ag^+ (irrev.); Anal. Calcd. for $C_{48}H_{52}N_4O_3$•0.5EtOAc: C 77.29, H 7.26, N 7.21. Found: C 77.19, H 7.25, N 7.34.

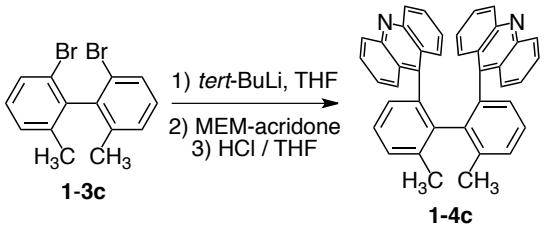

1-3c **1-4c**

Preparation of 6,6'-dimethylbiphenyl-2,2'-diyl-(9-acridine) **1-4c**

To a solution of 2,2'-dibromo-6,6'-dimethylbiphenyl **1-4c**[5] (370 mg, 1.09 mmol) in dry THF (14 mL) was added dropwise *tert*-BuLi (1.65 mol/L in pentane, 2.6 mL, 4.29 mmol) at -78 ˚C under Ar, and the mixture was stirred for 1 h at this temperature. Then, to the resulting suspension was added MEM-acridone (MEM-acridone) (624 mg, 2.20 mmol) at -78 ˚C. The mixture was allowed to warm and then stirred for 15 h at 24 ˚C. After addition of water, the resultant mixture was extracted with $CHCl_3$, then the organic layer was washed with brine and then concentrated. The residue was suspended in THF (14 mL), and 6 mol/L HClaq (14 mL). was added, and the mixture was stirred at 24 ˚C for 20 h. The resulting mixture was neutralized with 3 mol/L NaOHaq. and extracted with $CHCl_3$. The organic layer was washed with H_2O and brine, and dried over Na_2SO_4. Evaporation of solvent followed by chromatographic purification (SiO_2, EtOAc) afforded diacridine **1-4c** as a pale yellow solid (407 mg) in 66% yield.

Data for **1-4c**: m.p: 253 ˚C - 260 ˚C (decomp.); ^{1}H NMR (300 MHz, $CDCl_3$) δ 8.05 (2H, d, J = 8.6 Hz), 7.63 (2H, dd, J = 8.6 Hz, 8.6 Hz), 7.62 (2H, d, J = 7.7 Hz), 7.58 (2H, d, J = 8.6 Hz), 7.43 (2H, d, J = 7.7 Hz), 7.34 (2H, br-dd, J = 7.7 Hz, 7.7 Hz), 7.25 (2H, br-dd, J = 7.7 Hz, 7.7 Hz), 7.15 (2H, dd, J = 7.7 Hz, 7.7 Hz), 6.61 (2H, d, J = 7.7 Hz), 6.57 (2H, br-dd, J = 7.7 Hz, 7.7 Hz), 5.56 (2H, d, J = 7.7 Hz), 2,63 (6H, s); ^{13}C NMR (75 MHz, $CDCl_3$) δ 148.13, 147.55, 146.55, 139.02, 138.34, 135.50, 132.10, 130.60, 129.30, 129.25, 129.12, 127.10, 126.72, 126.37, 125.27, 124.30, 124.25, 123.82, 77.21, 21.10; IR (KBr) ν cm^{-1} 3063, 3045, 2995, 2918, 1628, 1607, 1556, 1539, 1517, 1460, 1437, 1411, 1378, 1262, 1142, 1011, 796, 787, 755, 740, 659, 644, 620; FD-LR-MS m/z 536 (M^+, BP); FD-HR-MS calcd. For $C_{40}H_{28}N_2$: 536.2252; found: 536.2253.

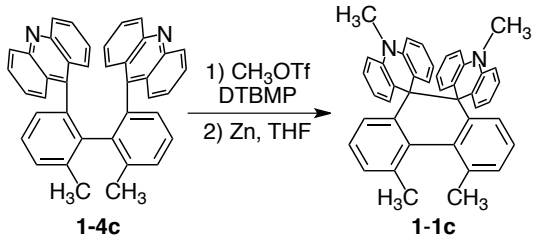

Preparation of 4',5'-dimethyldispiro[(10-methylacridan)-9,10'(9'*H*,10'*H*)-phenanthrene-10', 9''-(10''-methylacridan)] **1-1c**

To a solution of diacridine **1-4c** (199 mg, 0.370 mmol) and 2,6-di-*tert*-butyl-4-methylpyridine (DTBMP) (100 μL, 148 mg, 0.720 mmol) in dry CH_2Cl_2 (10 mL) was added dropwise methyl trifluoromethanesulfonate (2200 μL, 319 mg, 1.94 mmol) at 24 ˚C under Ar, and the mixture was stirred at this temperature for 21 h. The mixture was diluted with dry Et_2O. Filtration of the resulting yellow solid gave crude mixture containing **1-2c**$^{2+}$(TfO^-)$_2$, which was directly used for the further transformation.

To a solution of the crude dication salt in dry THF (20 mL) was added Zn powder (826 mg, 12.6 mmol) at 24 ˚C under Ar, and the mixture was stirred at this temperature for 7 h. After addition of water, the suspension was extracted with CH_2Cl_2. Then, the organic layer was washed with brine and dried over Na_2SO_4. After evaporation of solvent, the residue was purified by flash chromatography (Al_2O_3, hexane : CH_2Cl_2 = 5 : 1). The solid residue was washed with hexane and dried *in vacuo* to give **1-1c** (65.1 mg) as a colorless powder in 31% yield over 2 steps.

Data for **1-1c**: m.p: 260 ˚C - 270 ˚C (decomp.); ^{1}H NMR (300 MHz, $CDCl_3$) δ 7.20 (2H, d, J = 7.3 Hz), 7.04 (2H, dd, J = 7.3 Hz), 6.96 (2H, dd, J = 7.9 Hz, 7.9 Hz), 6.86 (2H, d, J = 7.3. Hz), 6.83 (2H, d, J = 7.9 Hz), 6.53 (2H, d, J = 7.9 Hz), 6.48 (2H, dd, J = 7.9 Hz, 7.9 Hz), 6.41 (2H, d, J = 7.9.1 Hz), 6.20 (2H, d, J = 7.9. Hz), 5.71 (2H, d, J = 7.9. Hz), 2.68 (6H, s), 2.58 (6H, s); ^{13}C NMR (75 MHz, $CDCl_3$) δ 133.20, 143.97, 142.81, 136.50, 133.82, 132.75, 131.77, 129.35, 128.23, 127.15, 127.05, 126.46, 125.67, 125.17, 118.89, 116.59, 111.92, 110.00, 58.85, 33.84, 20.97; IR (KBr) ν cm^{-1} 3038, 2883, 2820, 1737, 1607, 1591, 1470, 1362, 1325, 1292, 1273, 1246, 1195, 1165, 1134, 1099, 1059, 891, 861, 783, 773, 750, 732, 696, 655, 633; FD-LR-MS *m*/*z* 566 (M^+, BP), 283 (M^{2+}, 13); FD-HR-MS calcd. for $C_{42}H_{34}N_2$: 566.2722; found: 566.2731. Anal. calcd. for $C_{42}H_{34}N_2$•0.5H_2O: C, 87.62; H, 6.13; N, 4.87. Found: C, 87.45; H, 6.07; N, 4.74.

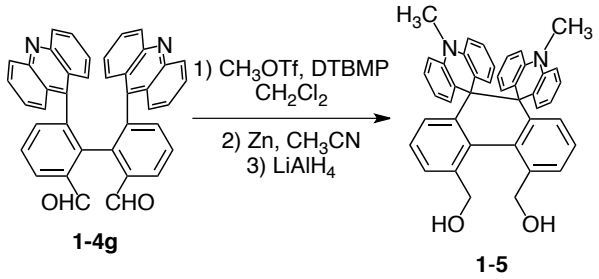

1-4g **1-5**

Preparation of dispiro[(10-methylacridan)-9,9'(10'H)-phenanthrene-10',9''-(10''-methylacridan)]-4',5'-dimethanol **1-5** via known compound **1-1g**[1k]

In the preparation of **1-5**, the known compound **1-1g** was generated from **1-4g**. To a solution of 6,6'-diformylbiphenyl-2,2'-di(9-acridine) **1-4g**[1k] (515 mg, 0.913 mmol) and DTBMP (379 mg, 1.84 mmol) in dry CH_2Cl_2 (20 mL) was added dropwise methyl trifluoromethanesulfonate (360 μL, 520 mg, 3.18 mmol) at 24 ˚C under Ar, and the mixture was stirred at this temperature for 14 h. The mixture was diluted with dry Et_2O. Filtration of the resulting yellow solid gave a crude mixture (644 mg) containing **1-2g**$^{2+}$(TfO^-)$_2$, which was directly used for the further transformation.

To a solution of the crude dication salt in CH_3CN (50 mL) was added Zn powder (1.80 g, 27.5 mmol) at 26 ˚C under Ar, and the mixture was stirred at this temperature for 20 min. After addition of water, the suspension was extracted with CH_2Cl_2. Then, the organic layer was washed with brine and dried over Na_2SO_4. Evaporation of solvent gave crude material of **1-1g** (407 mg) as a brown powder. This material was also used for further transformation without purification.

To a suspension of lithium aluminium hydride (179 mg, 4.73 mmol) in dry THF 40 mL was added a 20 mL THF solution of crude **1-1g** at 0 ˚C under Ar. The mixture was allowed to warm up and stirred for 2 h. After addition of saturated potassium sodium tartrate aqueous solution, the mixture was stirred until aluminium complex dissolved. The resultant mixture was extracted with CH_2Cl_2, then the organic layer was washed with brine and dried over Na_2SO_4. Chromtatographic purification (Al_2O_3, CH_2Cl_2 to CH_2Cl_2:CH_3OH = 20:1) gave **1-5** as a pale brown powder (333 mg) in 61% yield over 3 steps from starting diacridine **1-4g**.

Data for **1-5**: m.p: 192 ˚C - 196 ˚C (decomp.); ^{1}H NMR (300 MHz, $CDCl_3$) δ 7.57 (2H, d, J = 6.8 Hz), 7.21 (2H, dd, J = 6.8 Hz, J = 6.8 Hz,), 7.04 (2H, d, J = 6.8 Hz), 6.98 (4H, br-dd, J = 8.6 Hz, 8.6 Hz), 6.82 (2H, d, J = 8.6 Hz), 6.56 (2H, d, J = 8.6 Hz), 6.48 (2H, dd, J = 8.6 Hz, 8.6 Hz), 6.43 (2H, d, J = 8.6 Hz), 6.21 (2H, dd, J = 8.6 Hz, 8.6 Hz),

5.67 (2H, d, J = 8.6 Hz), 4.82-4.95 (4H, m), 2.70 (6H, s); ^{1}H NMR (300 MHz, dimethylsulfoxide (DMSO)-d_6) δ 7.51 (2H, d, J = 7.5 Hz), 7.17 (2H, dd, J = 7.5 Hz, 7.5 Hz), 6.98 (2H, dd, J = 8.4 Hz, 8.4 Hz), 6.94 (2H, dd, J = 8.4 Hz, 8.4 Hz), 6.80 (2H, d, J = 8.4 Hz), 6.75 (2H, d, J = 7.5 Hz), 6.46 (2H, d, J = 8.4 Hz), 6.43 (2H, dd, J = 8.4 Hz, 8.4 Hz), 6.09 (2H, dd, J = 8.4 Hz, 8.4 Hz), 5.52 (2H, d, J = 8.4 Hz), 5.20 (2H, br-dd, J = 5.3 Hz, 5.3 Hz), 4.76 (2H, dd, J = 12.1 Hz, 5.3 Hz), 4.56 (2H, dd, J = 12.1 Hz, 5.3 Hz), 3.32 (6H, s); ^{13}C NMR (75 MHz, DMSO-d_6) δ 143.59, 143.06, 138.66, 133.84, 131.70, 131.57, 129.99, 127.15, 127.07, 126.94, 126.84, 124.91, 124.06, 119.93, 116.17, 112.06, 110.49, 61.35, 58.08, 33.73; IR (KBr) ν cm^{-1} 3545, 3059, 2964, 2883, 1591, 1474, 1445, 1362, 1322, 1291, 1271, 1163, 1133, 1055, 1030, 992, 981, 796, 755, 732, 700, 655; FD-LR-MS m/z 598 (M^+, BP), 299 (M^{2+}, 15); Anal. calcd. for $C_{42}H_{34}N_2O_2$•CH_2Cl_2: C, 75.54; H, 5.31; N, 4.10. Found: C, 75.39; H, 5.51; N, 4.05.

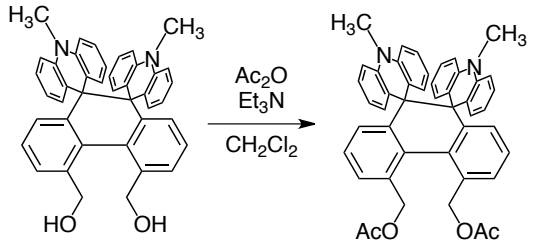

1-5 **1-1d**

Preparation of acetate **1-1d**

To a solution of **1-5** (91.9 mg, 0.153 mmol) and 4-dimethylaminopyridine (DMAP) (2.3 g, 23 μmol) in dry CH_2Cl_2 5 mL were added Et_3N (120 μL, 0.715 mmol) and acetic anhydride (33 μL, 0.349 mmol) at 27 ˚C, and the mixture was stirred for 4 h at this temperature. After addition of water, the resultant mix ture was extracted with CH_2Cl_2, then the organic layer was washed with water and brine, then dried over Na_2SO_4. Chromtatographic purification (Al_2O_3, hexane : CH_2Cl_2 = 3 : 1 0.5% v/v Et_3N, to hexane : CH_2Cl_2 = 1:1) gave **1-1d** as a pale green powder (66.0 mg) in 63% yield.

Data for **1-1d**: m.p.: 248 ˚C-256 ˚C (decomp.); ^{1}H NMR (300 MHz, $CDCl_3$) δ 7.43 (2H, d, J = 7.7 Hz), 7.19 (2H, dd, J = 7.7 Hz, J = 7.7 Hz), 7.07 (2H, d, J = 7.7 Hz), 6.98 (4H, dd, J = 7.0 Hz, J = 7.0 Hz), 6.89 (2H, d, J = 7.0 Hz), 6.56 (2H, d, J = 7.0 Hz), 6.49 (2H, dd, J = 7.0 Hz, 7.0 Hz), 6.43 (2H, d, J = 7.0 Hz), 6.17 (2H, dd, J = 7.0 Hz, 7.0 Hz), 5.67 (2H, d, J = 7.0 Hz), 5.43 (2H, d, J = 12.1 Hz). 5.34 (2H, d, J = 12.1 Hz), 2.70 (6H, s), 2.10 (6H, s); ^{13}C NMR (75 MHz, $CDCl_3$) δ 170.78, 144.20, 144.15, 142.72, 135.07, 132.46, 131.96, 131.65, 128.28, 127.66, 127.33, 127.26, 125.11, 124.56, 119.06, 116.77, 112.04, 110.16, 64.67, 55.67, 33.86, 21.07; IR (KBr) ν cm^{-1}; 3059, 2965, 2872, 2189, 1740, 1372, 1608, 1591, 1475, 1444, 1430, 1379, 1273, 1257, 1233, 1030, 1020, 756, 746, 733, 700; FD-LR-MS m/z 682 (M^+, BP), 341 (M^{2+}, 12); FD-HR-MS calcd. for $C_{46}H_{38}N_2O_4$: 682.2832; found: 682.2822.

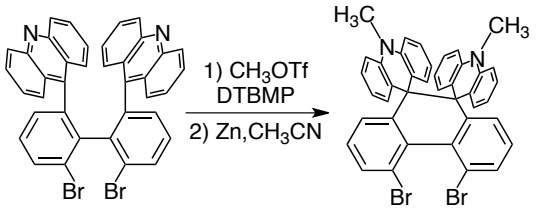

1-4e **1-1e**

Preparation of 4',5'-dibromodispiro[(10-methylacridan)-9,10'(9'*H*,10'*H*)-phenanthrene-10', 9''-(10''-methylacridan)] **1-1e**

To a solution of diacridine **1-4e**[2] (634 mg, 0.951 mmol) and DTBMP (270 μL, 397 mg, 1.93 mmol) in dry CH_2Cl_2 (30 mL) were added dropwise methyl trifluoromethanesulfonate (650 μL, 943 mg, 1.93 mmol) at 24 ˚C under Ar, and the mixture was stirred at this temperature for 15 h. The mixture was diluted with dry Et_2O. Filtration of the resulting yellow solid gave a crude mixture containing **1-2e**$^{2+}$(TfO^-)$_2$, which was directly used for the further transformation.

To a solution of the crude dication salt in dry CH_3CN (30 mL) was added Zn powder (3.10 g, 47.5 mmol) at 24 ˚C under Ar, and the mixture was stirred at this temperature for 17 h. After addition of water, the suspension was extracted with CH_2Cl_2. Then, the organic layer was washed with brine and dried over Na_2SO_4. After evaporation of solvent, the residue was purified by flash chromatography (Al_2O_3, hexane : CH_2Cl_2 = 4 : 1). The solid residue was washed with hexane and dried *in vacuo* to give **1-1e** (65.1 mg) as a pale yellow powder in 37% yield over 2 steps.

Data for **1-1e**: m.p: 263 ˚C - 276 ˚C (decomp.); ^{1}H NMR (300 MHz, $CDCl_3$) δ 7.60 (2H, dd, J = 0.74 Hz, 6.4 Hz), 6.97-7.04 (8H, m), 6.88 (2H, d, J = 7.9 Hz), 6.61 (2H, dd, J = 7.9 Hz, 7.9 Hz), 6.56 (2H, d, J = 7.9 Hz), 6.45 (2H, d, J = 7.9 Hz), 6.22 (2H, dd, J = 7.9 Hz, 7.9 Hz), 5.64 (2H, dd, J = 7.9 Hz), 2.69 (6H, s); ^{13}C NMR (75 MHz, $CDCl_3$) δ 145.92, 144.16, 142.78, 136.58, 132.37, 131.54, 131.39, 130.63, 128.51, 127.62, 127.56, 124.29, 121.64, 119.44, 1116.85, 112.17, 110.31, 77.21, 59.14, 33.84; IR (KBr) ν cm^{-1} 3048, 3008, 2965. 2882, 2817, 1590, 1471, 1362, 1273, 751, 724; FD-LR-MS *m*/*z* 698 ([M+4]$^+$, 59), 696 ([M+2]$^+$, bp), 694 (M$^+$, 48), 349 ([M+4]$^{2+}$, 8.6), 348 ([M+2]$^{2+}$, 15), 347 (M^{2+}, 7.4); FD-HR-MS calcd. for $C_{40}H_{28}Br_2N_2$: 694.0619; found: 694.0596.

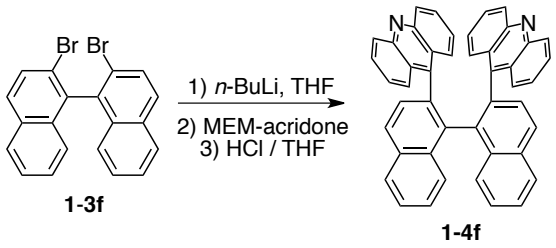

1-3f **1-4f**

Preparation of 1,1'-binaphthyl-2,2'-diyl-(9-acridine) **1-4f**

To a solution of 2,2'-dibromo-1,1'-binaphtyl **1-3f** (513 mg, 1.24 mmol) in dry THF (7 mL) was added dropwise *n*-BuLi (1.64 mol/L in hexane, 1.8 mL, 2.95 mmol) at -78 ˚C under Ar, and the mixture was stirred for 50 min. at this temperature. Then, to the resulting suspension was added MEM-acridone (1.05 g, 3.71 mmol) at -78 ˚C. The mixture was allowed to warm and then stirred for 15 h at 24 ˚C. After addition of water, the resultant mixture was extracted with $CHCl_3$, then the organic layer was washed with brine and then concentrated. The residue was suspended in THF, and 4 mol/L HClaq. was added, and the mixture was stirred at 24 ˚C for 27 h. The resulting mixture was neutralized with saturated $NaHCO_3$aq. and extracted with $CHCl_3$. The organic layer was washed with brine, dried over Na_2SO_4. Evaporation of solvent followed by chromatographic purification (SiO_2, $CHCl_3$: EtOAc = 1:1 to EtOAc) afforded diacridine **1-4f** as a pale yellow solid (444 mg) in 54% yield.

Data for **1-4f**: m.p: > 300 ˚C; ^{1}H NMR (300 MHz, $CDCl_3$) δ 7.97 (4H, dd, J = 8.6 Hz, 8.6 Hz), 7.80 (2H, d, J = 7.7 Hz), 7.68 (4H, d, J = 8.6 Hz), 7.64 (2H, dd, J = 8.6 Hz, 8.6 Hz), 7.62 (2H, d, J = 7.7 Hz), 7.51 (2H, dd, J = 8.6 Hz, 8.6 Hz), 7.41 (2H, dd, J = 7.7 Hz, 7.7 Hz), 7.34 (2H, dd, J = 7.7 Hz, 7.7 Hz), 7.00 (2H, d, J = 8.6 Hz), 6.53-6.59 (4H, m), 5.53 (2H, d, J = 8.6 Hz); ^{13}C NMR (400 MHz, $CDCl_3$) δ 149.99, 147.36, 146.10, 135.43, 134.23, 134.10, 133.15, 131.52, 129.46, 129.28, 129.22, 128.92, 128.84, 128.51, 128.01, 127.03, 126.48, 126.42, 125.99, 125.41, 124.13, 124.10, IR (KBr) ν cm^{-1} 3062, 2923, 1558, 1540, 1516, 1502, 1460, 1437, 1412, 819, 753, 686, 645; FD-LR-MS m/z 608 (M^+, bp), 304, (M^{2+}, 1.2); FD-HR-MS calcd. for $C_{46}H_{28}N_2$: 608.2253; found: 608.2258.

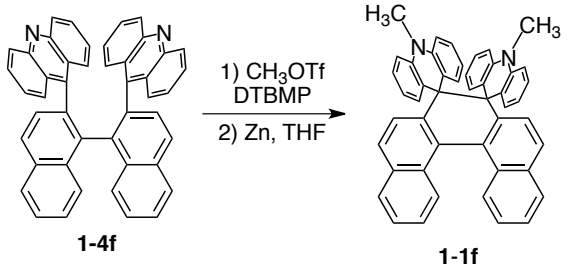

1-4f **1-1f**

Preparation of dispiro[(10-methylacridan)-9,3'(4H)-dibenzo[c,g]phenanthrene-4',9''-(10''-methylacridan)] **1-1f**

To a solution of diacridine **1-4f** (109 mg, 0.179 mmol) and 2,6-di-*tert*-butyl-4-methylpyridine (46 μL, 67.9 mg, 0.330 mmol) in dry CH_2Cl_2 (10 mL) was added dropwise methyl trifluoromethanesulfonate (100 μL, 145 mg, 0.883 mmol) at 22 ˚C under Ar, and the mixture was stirred at this temperature for 29 h. The mixture was diluted with dry Et_2O. Filtration of the resulting yellow solid gave crude mixture containing **1-2f**$^{2+}$(TfO^-)$_2$, which was directly used for the further transformation.

To a solution of the crude dication salt in dry THF (10 mL) was added Zn powder (224 g, 3.43 mmol) at 24 ˚C under Ar, and the mixture was stirred at this temperature for 19 h. After addition of water, the suspension was extracted with CH_2Cl_2. Then, the organic layer was washed with brine and dried over Na_2SO_4. Evaporation of solvent followed by chromatographic purification (Al_2O_3, hexane : EtOAc = 15 : 1 to CH_2Cl_2) afforded **1-1f** (62.2 mg) as a pale yellow powder in 54% yield over 2 steps.

Data for **1-1f**: m.p. > 300 ˚C, ^{1}H NMR (300 MHz, $CDCl_3$) δ 7.86 (2H, d, J = 8.4 Hz), 7.67 (2H, d, J = 8.4 Hz), 7.56 (2H, d, J = 8.4 Hz), 7.51 (2H, dd, J = 8.4 Hz, 8.4 Hz), 7.31 (2H, dd, J = 8.4 Hz, 8.4 Hz), 7.22 (2H, d, J = 8.4 Hz), 7.00 (2H, dd, J = 7.0 Hz, 7.0 Hz), 6.99 (2H, d, J = 7.0 Hz), 6.91 (2H, dd, J = 7.0 Hz, 7.0 Hz), 6.62 (2H, d, J = 7.0 Hz), 6.42 (2H, d, J = 7.0 Hz), 6.31 (2H, dd, J = 7.0 Hz, 7.0 Hz), 6.16 (2H, dd, J = 7.0 Hz, 7.0 Hz), 5.63 (2H, d, J = 7.0 Hz), 2.75 (6H, s); ^{13}C NMR (300 MHz, $CDCl_3$) δ 144.16, 142.88, 140.72, 132.64, 132.52, 131.78, 129.79, 129.74, 127.94, 127.67, 127.36, 127.24, 127.18, 125.52, 124.98, 124.83, 124.52, 119.30, 116.99, 112.17, 110.20, 77.21, 59.18, 33.84; IR (KBr) ν cm^{-1} 3058, 3001, 2967, 2869, 2818, 1606, 1589, 1502, 1472, 1362, 1325, 1273, 812, 747; FD-LR-MS m/z 638.4 (M^+, bp), 319 (M^{2+}, 10); FD-HR-MS calcd. for $C_{48}H_{34}N_2$: 638.2722; found: 638.2707.

X-ray analyses

Crystal data for **1-1b**•C_6H_6

Crystals were obtained by recrystallizing from C_6H_6/hexane. MF $C_{48}H_{38}N_2O$, FW 658.83, yellow block, 0.40 x 0.40 x 0.30 mm^3, monoclinic $C2/c$, a = 23.560(4), b = 11.900(2), c = 13.927(2) Å, β = 120.2315(5)°, V = 3373.5(9) $Å^3$, ρ (Z = 4) = 1.297 g cm^{-3}. A total of 3776 unique data ($2\theta_{max}$ = 55 °) were measured at T = 153 K by a Rigaku/MSC Mercury CCD apparatus (Mo Kα radiation, λ = 0.71070 Å). Numerical absorption correction was applied (μ = 0.77 cm^{-1}). The structure was solved by the direct method (SIR92) and refined by the full-matrix least-squares method on F^2 with anisotropic temperature factors for non-hydrogen atoms All the hydrogen atoms were located at the calculated positions and refined with riding. The final $R1$ and R_w values are 0.047 ($I > 2.0\sigma I$) and 0.140 (all data) for 3776 reflections and 231 parameters. Estimated standard deviations are 0.001-0.004 Å for bond lengths and 0.06-0.3 ° for bond angles, respectively.

Crystal data for **1-1c**•$CHCl_3$

Crystals were obtained by recrystallizing from $CHCl_3$/hexane. MF $C_{43}H_{35}Cl_3N_2$, FW 658.83, colorless platelet, 0.50 x 0.20 x 0.10 mm^3, triclinic P-1, a = 9.539(2), b = 10.253(2), c = 19.077(4) Å, α = 94.613(3), β = 90.4991(10), γ = 117.523(4)°, V = 1647.0(6) $Å^3$, ρ (Z = 2) = 1.383 g cm^{-3}. A total of 7112 unique data ($2\theta_{max}$ = 55 °) were measured at T = 153 K by a Rigaku/MSC Mercury CCD apparatus (Mo Kα radiation, λ = 0.71070 Å). Numerical absorption correction was applied (μ = 3.140 cm^{-1}). The structure was solved by the direct method (SIR2004) and refined by the full-matrix least-squares method on F^2 with anisotropic temperature factors for non-hydrogen atoms All the hydrogen atoms were located at the calculated positions and refined with riding. The final $R1$ and R_w values are 0.0996 ($I > 2.0\sigma I$) and 0.1063 (all data) for 7101 reflections and 434 parameters. Estimated standard deviations are 0.003-0.006 Å for bond lengths and 0.17-0.3 ° for bond angles, respectively.

Crystal data for **1-1d**

Crystals were obtained by recrystallizing from CH_2Cl_2/hexane. MF $C_{46}H_{38}N_2O_4$, FW 682.80, colorless needle, 0.40 x 0.050 x 0.030 mm^3, monoclinic $P2_1/n$, a = 12.847(3), b = 14.904(3), c = 17.656(3) Å, β = 100.818(2), °, V = 3320.6(10) $Å^3$, ρ (Z = 4) = 1.366 g cm^{-3}. A total of 7865 unique data ($2\theta_{max}$ = 55 °) were measured at T = 153 K by a Rigaku/MSC Mercury CCD apparatus (Mo Kα radiation, λ = 0.71070 Å). Numerical absorption correction was applied (μ = 0.869 cm^{-1}). The structure was solved by the direct method (SIR2004) and refined by the full-matrix least-squares method on F^2 with anisotropic temperature factors for non-hydrogen atoms All the hydrogen atoms were located at the calculated positions and refined with riding. The final $R1$ and R_w values are 0.0562 ($I > 2.0\sigma I$) and 0.0666 (all data) for 7863 reflections and 470 parameters. Estimated standard deviations are 0.018-0.003 Å for bond lengths and 0.11-0.17 ° for bond angles, respectively.

Crystal data for **1-1e**•$2CH_2Cl_2$

Crystals were obtained by recrystallizing from CH_2Cl_2/hexane. MF $C_{41}H_{30}Br_2Cl_2N_2$, FW 781.40, yellow platelet, 0.30 x 0.30 x 0.030 mm^3, monoclinic $P2/c$, a = 19.235(4), b = 12.036(2), c = 14.145(3) Å, β = 95.459(2), °, V = 3259.8(9) $Å^3$, ρ (Z = 4) = 1.592 g cm^{-3}. A total of 7296 unique data ($2\theta_{max}$ = 55 °) were measured at T = 153 K by a Rigaku/MSC Mercury CCD apparatus (Mo Kα radiation, λ = 0.71070 Å). Numerical absorption correction was applied (μ = 26.925 cm^{-1}). The structure was solved by the direct method (SIR2004) and refined by the full-matrix least-squares method on F^2 with anisotropic temperature factors for non-hydrogen atoms All the hydrogen atoms were located at the calculated positions and refined with riding. The final $R1$ and R_w values are 0.0863 ($I > 2.0\sigma I$) and 0.0975 (all data) for 7296 reflections and 426 parameters. Estimated standard deviations are 0.004-0.011 Å for bond lengths and 0.3-0.5 ° for bond angles, respectively.

Crystal data for **1-1f**

Crystals were obtained by recrystallizing from $CHCl_3$/hexane. MF $C_{48}H_{34}N_2$, FW 638.81, yellow platelet, 0.20 x 0.20 x 0.150 mm^3, triclinic *P*-1, a = 9.668(9), b = 10.494(9), c = 17.86(2) Å, α = 97.323(13), β = 92.235(6), γ = 114.47(2)˚, V = 1627(3) $Å^3$, ρ (Z = 2) = 1.304 g cm^{-3}. A total of 5905 unique data ($2\theta_{max}$ = 55 ˚) were measured at T = 153 K by a Rigaku/MSC Mercury CCD apparatus (Mo Kα radiation, λ = 0.71070 Å). Numerical absorption correction was applied (μ = 0.752 cm^{-1}). The structure was solved by the direct method (SIR2004) and refined by the full-matrix least-squares method on F^2 with anisotropic temperature factors for non-hydrogen atoms All the hydrogen atoms were located at the calculated positions and refined with riding. The final $R1$ and R_w values are 0.1204 ($I > 2.0\sigma I$) and 0.1363 (all data) for 5905 reflections and 452 parameters. Estimated standard deviations are 0.005-0.09 Å for bond lengths and 0.3-0.6 ˚ for bond angles, respectively.

References

[1] a) T. Suzuki, J. Nishida, T. Tsuji, Angew. Chem. Int. Ed. Engl. 1997, 36, 1329.; b) J. Nishida, T. Suzuki, M. Ohkita, T. Tsuji, *Angew. Chem. Int. Ed.* **2001**, *40*, 3251.; c) T. Suzuki, R. Yamamoto, H. Higuchi, E. Hirota, M. Ohkita, T. Tsuji, *J. Chem. Soc. Perkin Trans. 2* **2002**, 1937.; d) T. Suzuki, J. Nishida, T. Tsuji, *Chem. Commun.* **1998**, 2193.; e)T. Suzuki, A. Migita, H. Higuchi, H. Kawai, K. Fujiwara, T. Tsuji, *Tetrahedron Lett.* **2003**, *44*, 6837.; f) T. Suzuki, S. Tanaka, H. Higuchi, H. Kawai, K. Fujiwara, *Tetrahedron Lett.* **2004**, *45*, 8563.; g) T. Suzuki, S. Tanaka, H. Kawai, K. Fujiwara, *Chem. Asian J.* **2007**, *2*, 171.; h) T. Suzuki, T. Iwai, E. Ohta, H. Kawai, K. Fujiwara, *Tetrahedron Lett.* **2007**, *48*, 3599.; i) T. Suzuki, K. Ohta, T. Nehira, H. Higuchi, E. Ohta, H. Kawai, K. Fujiwara, *Tetrahedron Lett.* **2008**, *49*, 772.; j) T. Suzuki, Y. Ishigaki, T. Iwai, H. Kawai, K. Fujiwara, H. Ikeda, Y. Kano, K. Mizuno, *Chem. Eur. J.* **2009**, *131*, 16896.; k) T. Suzuki, Y. Yoshimoto, K. Wada, T. Takeda, H. Kawai, K. Fujiwara, *Heterocycles* **2010**, *80*, 149.

[2] T. Suzuki, Y. Yoshimoto, T. Takeda, H. Kawai, K. Fujiwara, *Chem. Eur. J.* **2009**, *15*, 2210.

[3] R. Cosmo, T. W. Hambley, S. Sternhell, *J. Org. Chem.* **1987**, *52*, 3119.

[4] E. Osawa, P. M. Ivanov, C. Jaime, *J. Org. Chem.* **1983**, *48*, 3990.

[5] Q. Perron, A. Alexakis, *Adv. Synth. Catal.* **2010**, *352*, 2611.

Chapter 2
Construction of Novel Chiral-memory Unit Based on 9,9,10,10-tetraaryldihydrophenanthrene-type Dynamic Redox Systems

2-1 Introduction

2-1-1 Electrochiroptical response system based on dynamic redox system

In the author's laboratory, dynamic redox systems based on the 9,9,10,10-tetraaryldihydrophenanthrene skeleton have been studied from the viewpoint of novel electrochromic systems,[1] by which the electrochemical input is transduced into UV-Vis spectral output.[2] In these systems, the neutral electron donor is reversively converted into the biphenylic dication upon two electron oxidation accompanied by C_9-C_{10} bond cleavage.

As shown in Chapter 1, this skeleton adopts helical structure. In addition, the dication has the asymmetric element of axial chirality. Their stability of configuration depends on the structural features such as the substituents at the bay region. For instance, donors and dications without any substituent (R = H) can not be optically resolved because of their rapid ring flip/rotation. On the other hand, certain dibromo derivatives (R = Br; Ar_2C = spiro-9-xanthene) were successfully resolved[3](Scheme 2-1). This is also the case for the pairs of dihydro[5]helicene-binaphthylic dications.[4],[5] By using optically resolved compounds, their circular dichroism (CD) drastically changes upon redox reactions, so that they are the novel members of less well-developed electrochiroptical response systems.[3],[6]

Scheme 2-1

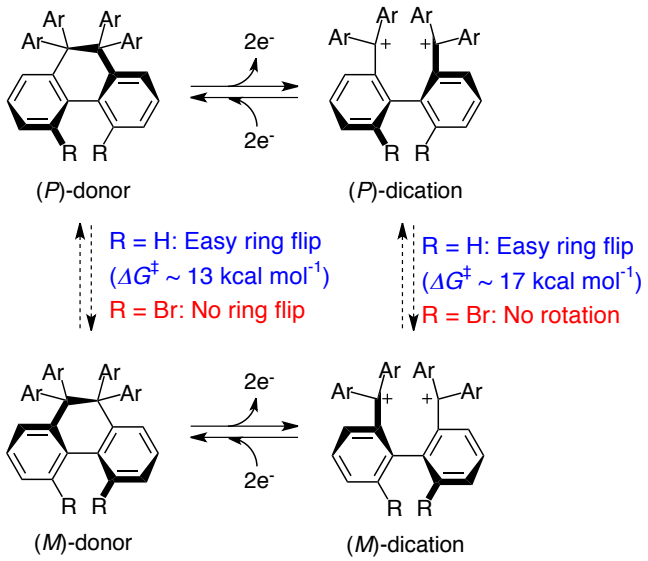

2-1-2 Molecular design of redox-type chiral memory

By adopting the concept of dynamic redox system, the author expected that the novel redox system with a function of chiral memory (Scheme 2-2) can be realized by fusing seven membered ring at the bay region of the original framework of dihydrophenanthrene. In this system, racemization barriers of the species would be drastically modified by redox reaction: the racemization would easily occur by ring flip in donor **2-1** (”erasable/writable state”), whereas the racemization of dication **2-2**$^{2+}$ would be suppressed (”memorizing state”) by large increase in steric repulsion between the bulky Ar_2C^+ units at the bay region. The dihydrophenanthroxepin-dihydrodibenzoxepin skeleton was selected as a first prototype to examine the concept in anticipation that the ether oxygen on the bridge would act as a Lewis basic part, to which a chiral Lewis acid could be bound to bias the helical preference in **2-1**. Such system can store the chiral information in the memorizing state (**2-2**$^{2+}$) and erase in the erasable/writable state (**2-1**). When chiral information of the external sources is successfully transmitted to the writable state of this memory unit, the enantiomeric ratio of **2-1** would be biased upon addition of the chiral sources, which could be memorized by oxidizing **2-1** to **2-2**$^{2+}$.

Scheme 2-2

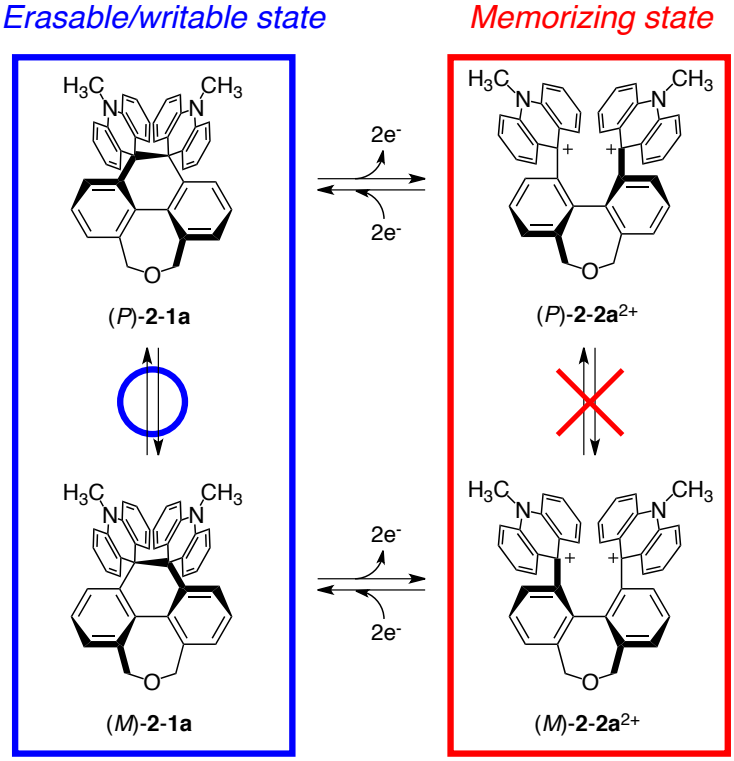

Erasing the memory would be done by reduction of optically active **2**-**2**$^{2+}$ into **2**-**1** of configurational instability.

The largest merit by using the dynamic redox system is suppressing electron exchange between the erasable/writable state (**2**-**1**) and the memorizing state (**2**-**2**$^{2+}$). In the conventional reversible redox systems, easy electron-exchange prevents them from being used as memory units (Scheme 2-3).

Scheme 2-3

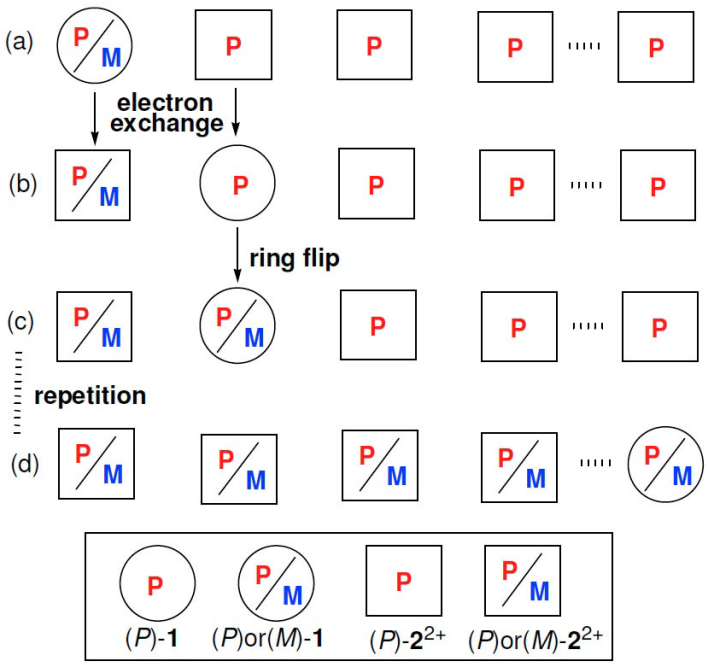

(a) Chiral information is stored in configurationally stable (*P*)-**2**-**2**$^{2+}$ molecules.

(b) Configurationally labile (*P*)-**2**-**1** is formed by electron-exchange.

(c) Ring flip of (*P*)-**2**-**1** furnishes partial loss of chiral information of the system.

(d) Repetition of the above process results in total racemization of **2**-**2**$^{2+}$.

In the present case, (a) -> (b) is prohibited by the electrochemical bistability.

2-2 Properties of 2-1a/2-2a^{2+}

2-2-1 Redox behavior

Firstly, redox behavior of **2-1a** and **2-2a**$^{2+}$, which is one of the key properties to realize the chiral memory unit, was investigated by cyclic voltammetry. According to the volammograms, **2-1a** undergoes irreversible 2e-oxidation at +0.04 V *vs.* Ag/Ag^{+} (E^{ox}). The return peak in the far cathodic region corresponds to the reduction process of **2-2a**$^{2+}$ (E^{red} = -0.43 V *vs.* Ag/Ag^{+}), which was confirmed by the separate measurement on **2-2a**$^{2+}$ salt (Figure 2-1). These redox potentials are close to those of the derivatives **2-1c**/**2-2c**$^{2+}$ without the fusing seven-membered ring measured under the similar conditions (Scheme 2-4).[7] The observed separation of redox potentials provides the present pairs with high electrochemical bistability to prevent the loss of chiral information stored in **2-2**$^{2+}$ even in the coexistence of **2-1** and **2-2**$^{2+}$. Such characteristics were later confirmed experimentally (*vide infra*).

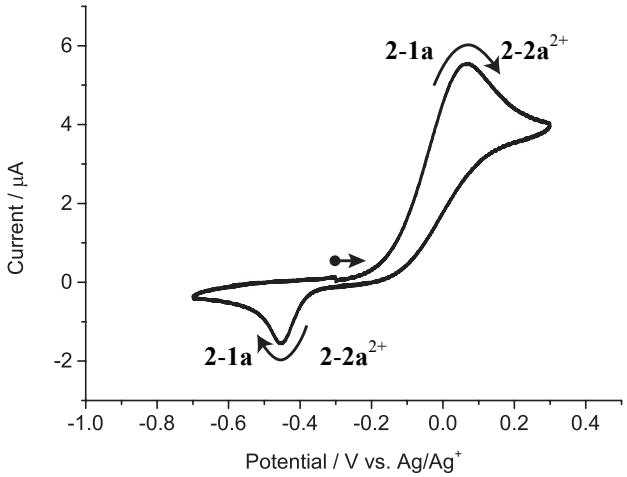

Figure 2-1. Cyclic voltammogram of 0.8 mM **2-1a** in 0.1 M Bu_4NClO_4 solution at scan rate of 100 mV s^{-1}. Pt working and counter electrodes were used.

Scheme 2-4

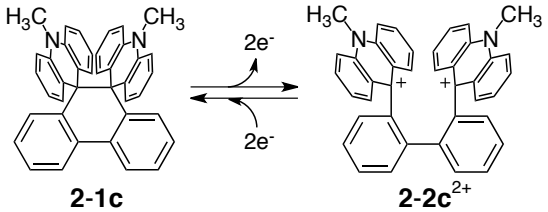

2-1c **2-2c**$^{2+}$

E^{ox} = +0.05 V *vs.* Ag/Ag^{+} E^{red} = -0.49 V *vs.* Ag/Ag^{+}

2-2-2 X-ray structure of 2-1/2-2a^{2+}

According to an X-ray analysis, the condensed heterocycle in **2-1a** adopts a helical structure, as shown in Chapter 1 (Figure 2-2). X-ray analysis of dication **2-2a**$^{2+}$ can also be carried out successfully. As expected, this dication also adopts a helical structure, whose torsion angle [50.8(3) ˚] is larger than that of **2-1a**, suggesting a larger energy barrier of helicity inversion of the dication (Figure 2-3).

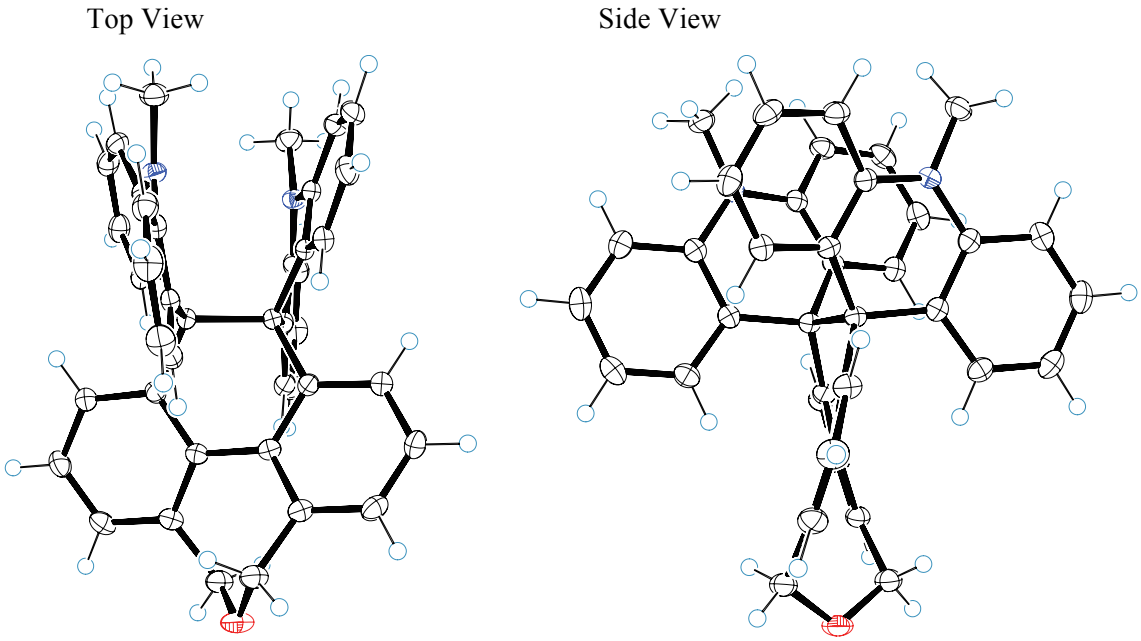

Figure 2-2. X-ray structure of **2-1a** in **2-1a**•C_6H_6 crystal

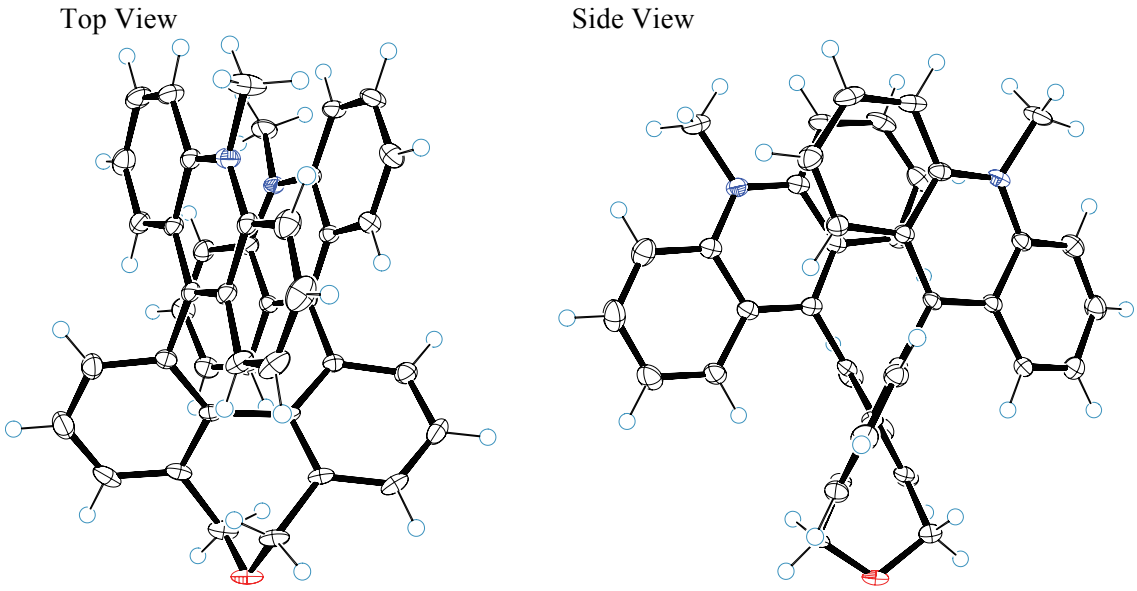

Figure 2-3. X-ray structure of dication **2-2a**$^{2+}$ in *rac*-**2-2a**$^{2+}$($SbCl_6^-$)$_2$•CH_3CN crystal

2-2-3 Preparation of optically active dications 2-2a^{2+} and chiropical properties

Racemization of dication **2-2a**$^{2+}$ was supposed to be suppressed by a larger steric repulsion than in **2-1a**. Therefore, preparation of optically active **2-2a**$^{2+}$ was planned and carried out as follows.

Dication precursor *rac*-**2-4a** were optically resolved by recycle-type chiral HPLC (SUMICHIRAL OA-2000 column, 25 ˚C; hexane : CH_2Cl_2 = 1, 0.5% Et_3N) (Figure 2-4). *M*-helical isomer (*M*)-**2-4a** was eluted as the first fraction, whose absolute configuration was determined by theoretical calculation.[8] It was converted to optically active dication **2-2a**$^{2+}$ as in the case of racemic compounds (Scheme 2-5).

Scheme 2-5

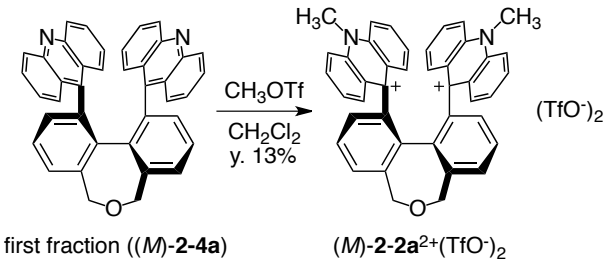

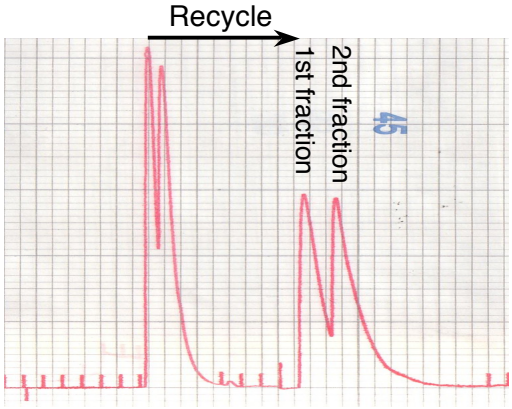

Figure 2-4. Chromatogram of *rac*-**2-4a** on SUMICHIRAL OA-2000 (hexane : CH_2Cl_2 = 1:1, 0.5 % Et_3N)

In the CD spectrum, optically pure salt of (*M*)-**2-2a**$^{2+}$(TfO^-)$_2$ showed a large negative couplet in the UV region [λ_{ext} 270 nm ($\Delta\varepsilon$ -36.4), 258 nm ($\Delta\varepsilon$ –33.0) in CH_3CN] (Figure 2-5), which is due to effective exciton coupling between the two acridinium moieties arranged in a helical configuration.

Figure 2-5. CD spectrum of optically pure (*M*)-**2-2a**$^{2+}$(TfO^-)$_2$ in CH_3CN

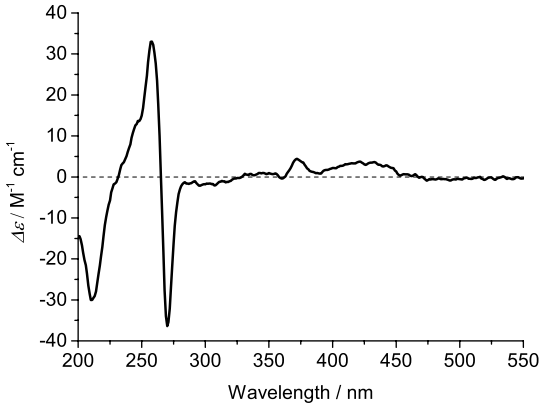

2-3 Behavior as chiral memory unit

2-3-1 Racemization barrier of 2-1a/2-2a^{2+}

For the investigation of properties of **2-1** and **2-2**$^{2+}$ as chiral memory unit, racemization barriers of **2-1a** and **2-2a**$^{2+}$ were estimated.

First, the estimation was carried out based on VT-NMR analyses. The NMR spectrum (CD_2Cl_2, 300 MHz) of **2-1a** showed two sharp resonances for the methylene protons at the seven-membered ring at -90 ˚C (4.78 and 4.36 ppm), which were coalesced upon warming to -15 ˚C (Figure 2-6a), corresponding to a $\Delta G^{\ddagger}$ value of 12.2 kcal mol^{-1} for the ring flip (T_c = 258 K, k = 7580 s^{-1} at 25 ˚C). Thus, **2-1a** is proven to act as an easily-racemized "erasable/writable"-state. Similar analyses of dication **2-2a**$^{2+}$ by VT-NMR spectra indicate that no coalescence occurs even at the higher temperature (Figure 2-6b), which only gave the value of lower limit for racemization barriers ($\Delta G^{\ddagger}$ > 20 kcal mol^{-1}).

Then, the estimation for the barriers of dication **2-2a**$^{2+}$ were carried out by CD spectral analyses. The CD spectra of optically active salts of dications **2-2a**$^{2+}$ did not show any decay over several days at 25 ˚C ($\Delta G^{\ddagger}$ > 25 kcal mol^{-1}), which confirmed the long-lasting chiral memory of this unit (Figure 2-5).

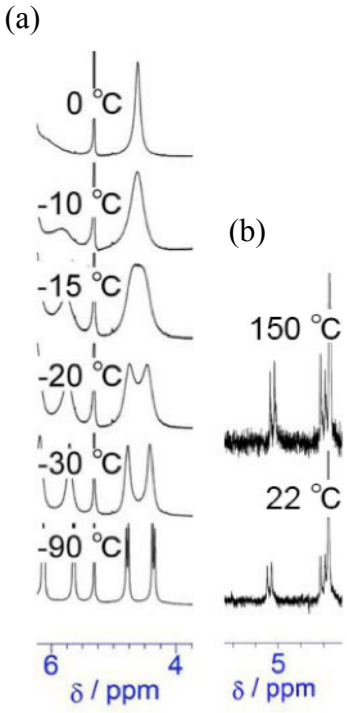

Figure 2-6. VT-NMR spectra of donor **2-1a** in CD_2Cl_2 and dication **2-2a**$^{2+}$ in DMSO-d_6

2-3-2 Spectral response of chiral memory unit

Erasing process of the present chiral memory unit was investigated by conducting electrolysis of optically pure dication (*M*)-**2**-**2a**$^{2+}$, and the changes were followed by three kinds of spectroscopy at 25 ˚C. The UV-Vis spectral changes during the conversion of **2**-**2a**$^{2+}$ into neutral donor **2**-**1a** exhibit several isosbestic points with a loss of absorptions in the visible region, which were regenerated upon reoxidation (Figure 2-7a). Fluorescence of (*M*)-**2**-**2a**$^{2+}$ was also lost upon reduction to **2**-**1a**, yet recovered completely upon reversal of the polarity of the electrodes (Figure 2-7b), which demonstrates clean interconversion between **2**-**1a** and **2**-**2a**$^{2+}$. In contrast, the CD signals of (*M*)-**2**-**2a**$^{2+}$ disappeared gradually upon reduction, and were not reproduced upon reoxidation (Figure 2-7c), which demonstrates that the resulting (*M*)-**2**-**1a** was easily racemized to lose chiral information. These findings successfully demonstrate electrochemical response of a novel chiral memory unit (”erasing”-process of chiral memory).

If the electron-exchange between **2**-**1a** and **2**-**2a**$^{2+}$ were a facile process, the CD signals should have shown a current-independent decay in the middle of electrolysis, but this was not the case (Figure 2-8). All of the these spectral changes coincide, showing that the loss of CD signal was induced only by the electrochemical consumption of configurationally stable (*M*)-**2**-**2a**$^{2+}$.

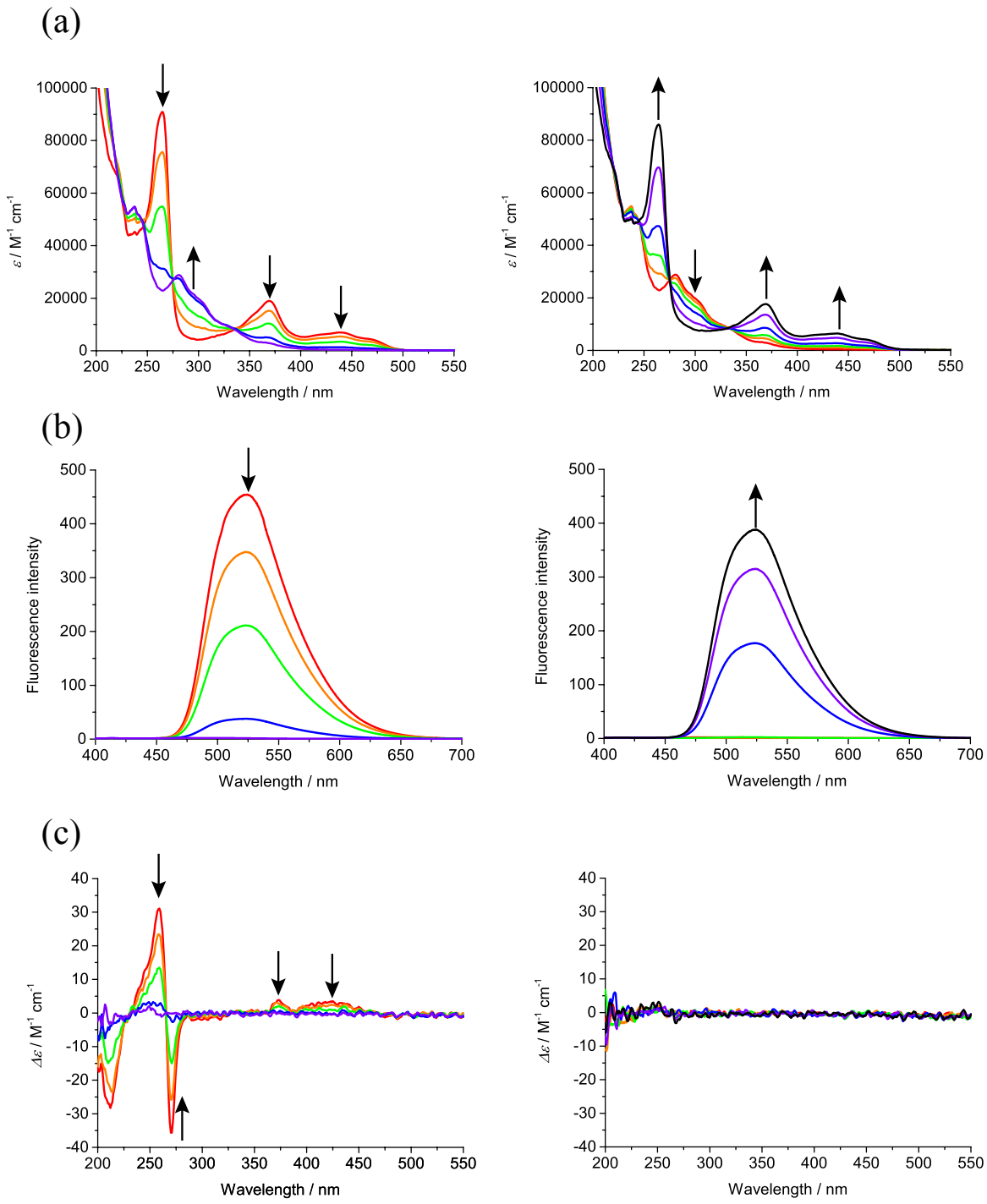

Figure 2-7. (left) Changes in the a) UV-Vis, b) fluorescence (λ_{exc} 370 nm), and c) CD spectra of (*M*)-**2**-**2a**$^{2+}$ (9.0 x 10^{-6} M) in CH_3CN (containing 0.05 M Et_4NClO_4) upon constant-current electrochemical reduction (37 μA at 2.5-min interval, at 25˚C). Figures on the right show the changes upon reoxidation of the as-prepared **2**-**1a** (37 μA at 3-min interval).

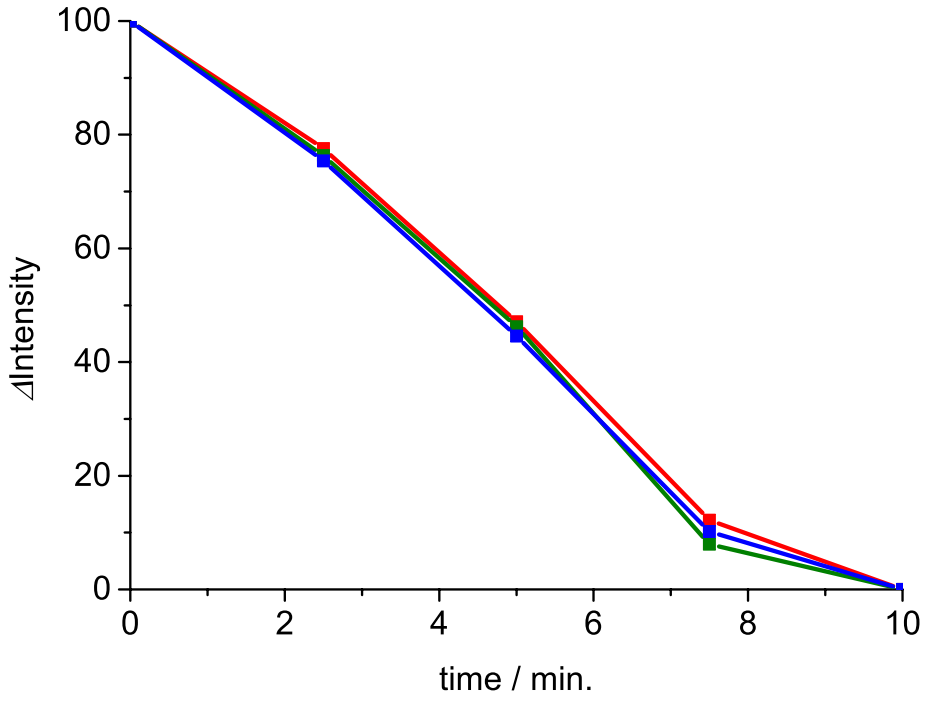

Figure 2-8. Time-courses of UV-Vis (changes of ε at 264.5 nm), fluorescence (changes of intensity at 524 nm), and CD (changes of $\Delta\varepsilon$ at 259 nm) spectra upon electrochemical reduction of (*M*)-**2**-**2a**$^{2+}$ salt.

2-3-3 Attempt of chiral induction

Finally, the writing-process of this chiral memory unit was investigated. Upon addition of suitable chiral guests such as chiral Lewis acids (LA*), enantiomeric ratio of donor (*P*)/(*M*)-**2**-**1** would be biased, if possibly, by preferred formation of one of the two diastereomeric complexes **2**-**1**-LA*. In such desirable conditions, the chiral information of LA* transferred into configurationally labile **2**-**1** would be memorized as configurationally stable dication **2**-**2**$^{2+}$ upon oxidation of as-prepared **2**-**1**-LA*.
In this work, several LA* shown in Scheme 2-6[9] were investigated, yet no induced CD was observed.

Scheme 2-6

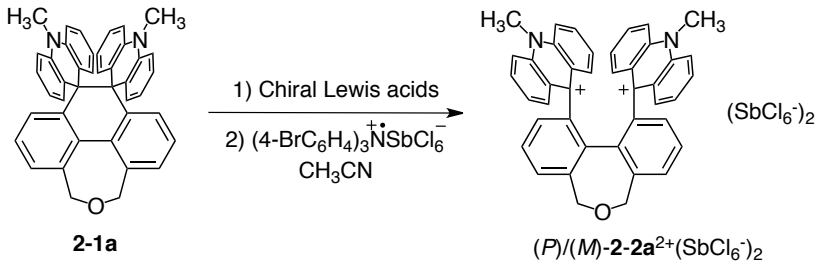

2-1a

(*P*)/(*M*)-**2**-**2a**$^{2+}$(SbCl$_6^-$)$_2$

Chiral Lewis acids:

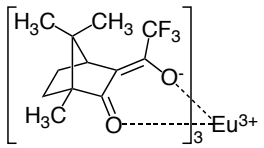

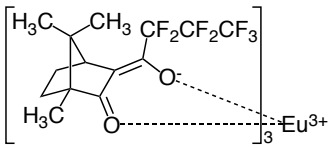

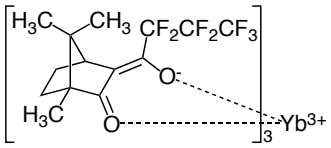

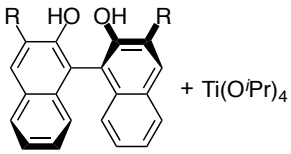

R = H, CH_3, Br

2-4 Construction of advanced system

2-4-1 Molecular design

To strengthen the interaction between donor **2-1** and LA*, interacting site of the bridging unit was replaced by the ester unit for the ether unit in **2-1a**, and the newly designed **2-1b**/**2-2b**$^{2+}$ would show similar chiral memory properties (Scheme 2-7).

Scheme 2-7

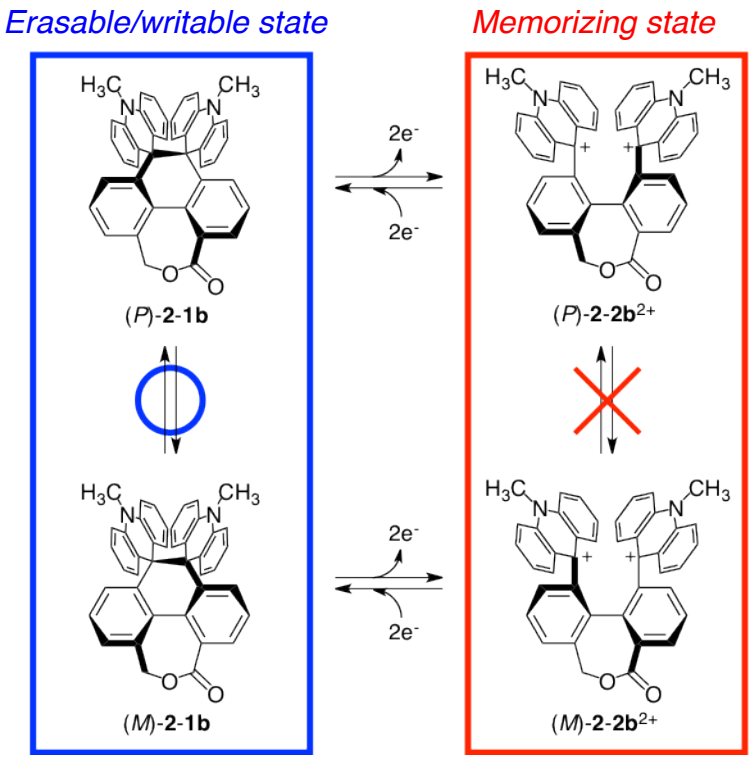

2-4-2 Preparation

Neutral donor **2-1b** and dication **2-2b**$^{2+}$ were prepared as shown in Scheme 2-8. Two formyl groups of *rac*-**2-5** were protected as cyclic acetals, and the resulting *rac*-**2-6** was dilithiated by *n*-BuLi followed by the reaction with MEM-acridone. Simultaneous deprotection of MEM groups and acetal groups under acidic conditions gave diacridine *rac*-**2-7**.[10] Canizzaro reaction of *rac*-**2-7** upon treatment of K_2CO_3 in CH_3OH gave lactone *rac*-**2-4c** in 70% yield. Under the presence of 2,6-di-*tert*-butyl-4-methylpyridine (DTBMP), *rac*-**2-4c** was methylated by CH_3OTf to give dication *rac*-**2-2b**$^{2+}$(TfO^-)$_2$ as a yellow solid, which contains a small amount of inpurity. Reduction of crude *rac*-**2-2b**$^{2+}$(TfO^-)$_2$ by Zn dust gave the neutral donor **2-1b** as a colorless powder in 49% yield over two steps. Reoxidation of donor **2-1c** with two equivalents of one electron

oxidizing agent $(4\text{-}BrC_6H_4)_3N^{+\cdot}SbCl_6^-$ regenerated dication salt *rac*-**2-2b**$^{2+}$ $(SbCl_6^-)_2$ in 85% yield.

Scheme 2-8

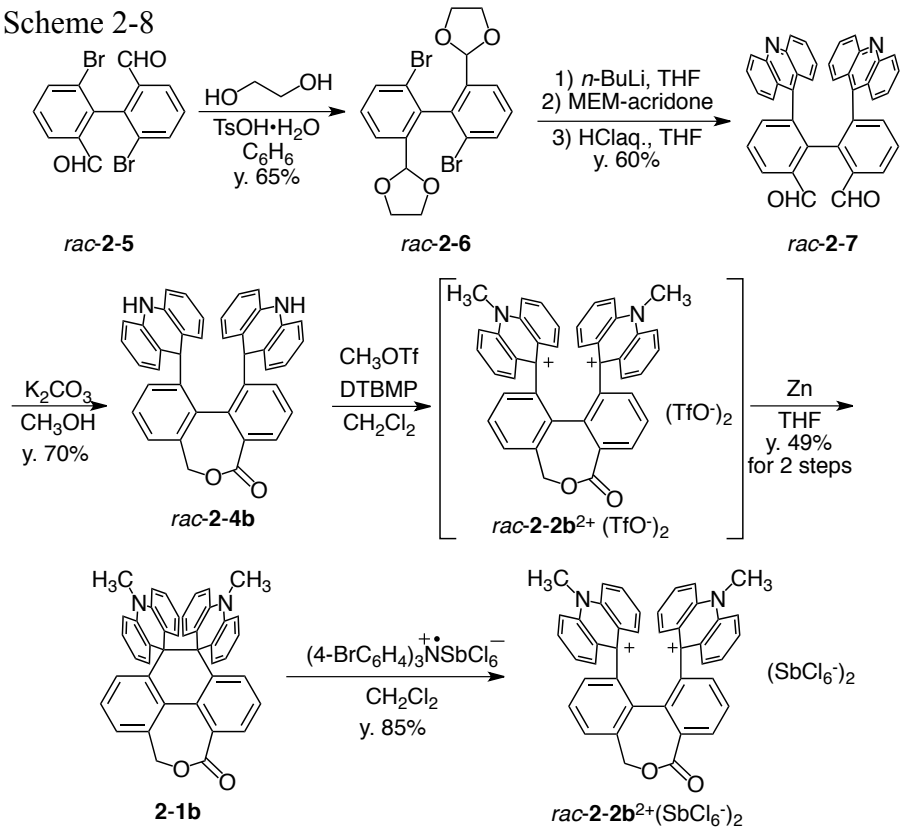

2-4-3 Redox behavior of 2-1b/2-2b^{2+}

According to the voltammetric analyses, the new redox pair of **2-1b** and **2-2b**$^{2+}$ shows similar dynamic redox behavior to **2-1a** and **2-2a**$^{2+}$ (Figure 2-9). The oxidation potential of **2-1b** (+0.55 V *vs.* Ag/Ag^+) is separated from the reduction potential of **2-2b**$^{2+}$ (+0.21 V *vs.* Ag/Ag^+) by 0.34 V, which may suppress the electron exchange between **2-1b** and **2-2b**$^{2+}$.

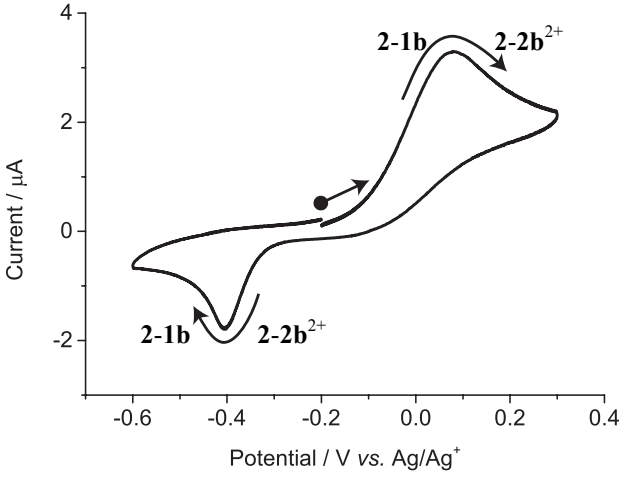

Figure 2-9. Cyclic voltammogram of 0.4 mM **2-1b** in 0.1 M Bu_4NBF_4 CH_2Cl_2 solution at scan rate of 100 mV s^{-1}. Pt working and counter electrodes were used.

2-4-4 Racemization barrier of 2-1b/2-2b^{2+}

Investigation of racemization barrier of **2-1b**/**2-2b**$^{2+}$ was carried out based on a VT-NMR analysis (Figure 2-10). The value of **2-1b** was estimated to be 17.7 kcal mol^{-1} (T_c = 313 K, k = 0.658 s^{-1} at 25 ˚C). As in the case of **2-2a**$^{2+}$, the spectrum of **2-2b**$^{2+}$ did not show coalescence up to 150 ˚C, which only indicated the lower limit of the value ($\Delta G^{\ddagger}$ > 21 kcal mol^{-1}).

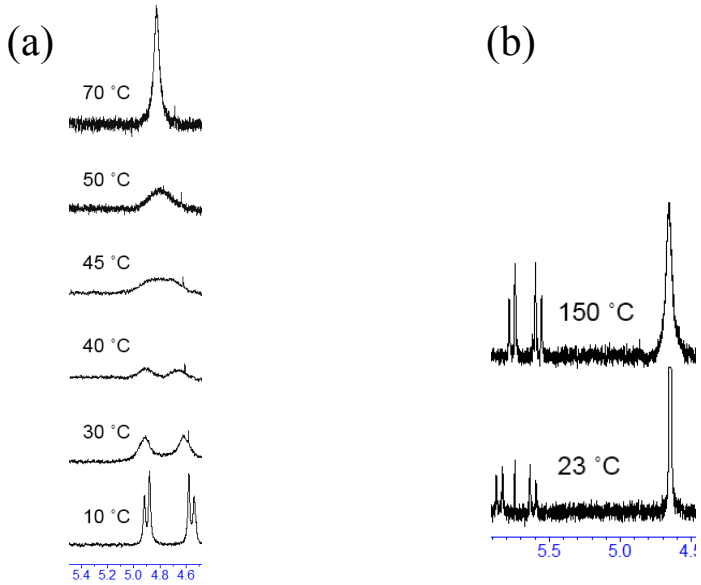

Figure 2-10. VT-NMR spectra of (a) donor **2-1b** in C_6D_6 and (b) dication **2-2b**$^{2+}$($SbCl_6^-$)$_2$ in DMSO-d_6.

2-4-5 Toward preparation of optically active 2-2b^{2+}

For further investigation of new dication **2-2b**$^{2+}$, preparation of optically active **2-2c**$^{2+}$ has been conducted as follows, which needs further investigation before completion.

First, optical resolution of dication precursor **2-4b** was carried out by recycle-type chiral HPLC (DAICEL CHIRALPAK IA, hexane : CH_2Cl_2 = 1 : 1, 0.5% v/v EtOH). Absolute configuration of the first fraction was determined by the CD spectrum. As in the case of ether-type precursor **2-4b**, the separation of the second fraction is imperfect due to tailing of the first peak. In the CD spectrum of the first fraction, similar pattern of Cotton effect to (*M*)-**2-4b** was observed for the first band. Since the negative couplet around 380 nm comes from the exciton coupling of two acridine chromophores, the

close similarity in CD spectrum suggests that the first fraction of **2-4b** is the (*M*)-enantiomer (Figure 2-12).

Due the by-production of inseparable impurity, methylation conditions of (*M*)-**2-4b** needs to be further investigated.

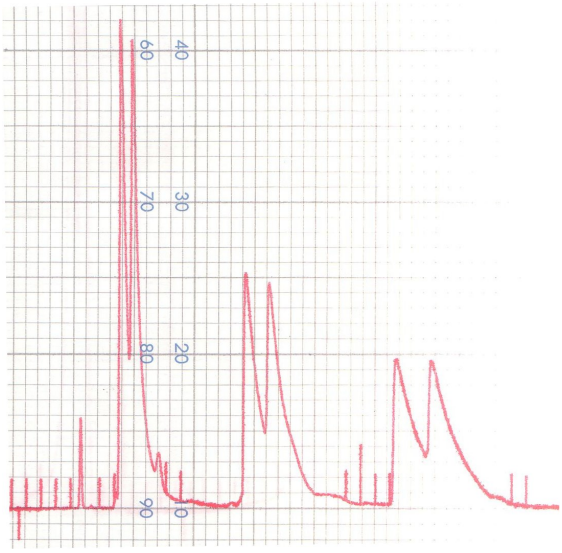

Figure 2-11. Chromatogram of *rac*-**2-4b** on DAICEL CHIRALPAK IA (hexane : CH_2Cl_2 = 1:1, 0.5 % EtOH)

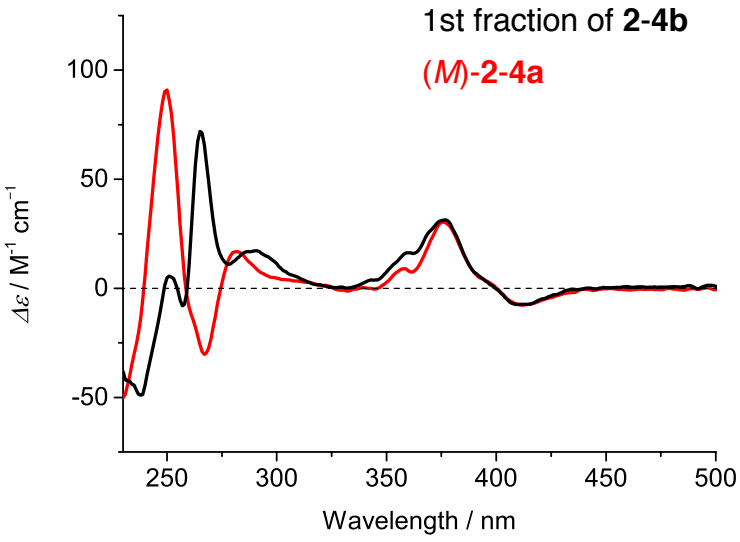

Figure 2-12. CD spectra of the first fraction of **2-4b** (black line) and (*M*)-**2-4a** (red line)

2-5 Summary

In this work, the novel redox-type chiral memory unit **2-1**/**2-2**$^{2+}$ was constructed (Scheme 2-9). In this system, racemization barriers are drastically changes upon redox reaction: racemization barrier in the neutral state is low enough to undergo facile racemization at room temperature, while the value is very high in the dicationic state to suppress racemization. Therefore, the present molecule can write/erase the chiral information in the neutral state and store it in the dicationic state. First, ether-bridged redox system (**a**) was prepared. Racemization barriers in neutral/dicationic state were determined by VT-NMR and/or CD spectral analyses. Erasing process of chiral memory unit was investigated by following the UV-Vis, fluorescence, CD spectral changes upon electrochemical reduction/reoxidation of (*M*)-**2a**$^{2+}$. Writing-process of the chiral memory with the ether-type bridging unit was found to be difficult, probably due to weak coordinating ablity toward chiral Lewis acid.

Then, another chiral memory unit **2-1b**/**2b**$^{2+}$ with the ester-type bridging unit was prepared to enhance coordinating ability toward Lewis acid. The new pair **2-1b**/**2b**$^{2+}$ also showed switching of racemization barriers upon redox reactions.

Scheme 2-9

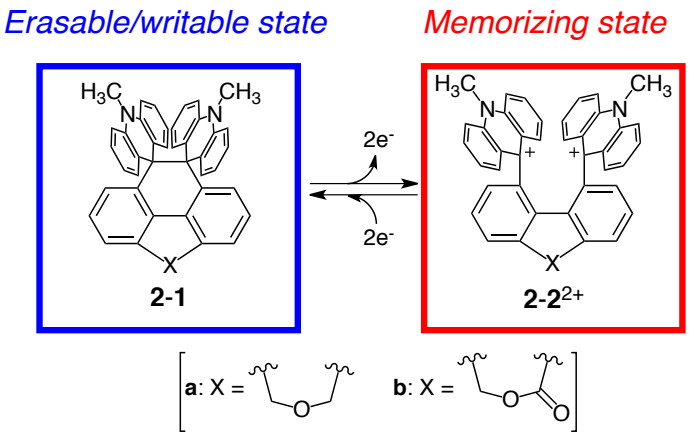

Experimental section

General

^{1}H and ^{13}C NMR spectra were recorded on a JEOL AL-300 (^{1}H 300 MHz and ^{13}C 75 MHz) spectrometer. Chemical shifts (δ) were reported with tetramethylsilane (TMS) (in $CDCl_3$ and dimethylsulfoxide (DMSO)-d_6, δ=0.00 ppm) or CH_3CN (in CD_3CN, δ=1.93 ppm) as internal standards. IR spectra were recorded on a JEOL WINSPEC100 infrared spectrophotometer. Mass spectra were recorded on a JMS-AX500 spectrometers in FD mode (GC-MS & NMR Laboratory, Graduate School of Agriculture, Hokkaido University). Elemental Analyses were taken on J-Science micro corder JM10 or on a Yanaco CHN corder MT-6 at the Instrumental Analysis Division, Equipment Management Center, Creative Research Institution, Hokkaido University. Cyclic voltammograms were measured with a BAS ALS-600A electrochemical analyzer. X-ray diffraction data for a single-crystal analyses were measured by a RIGAKU AFC-5R + Mercury CCD apparatus (50 kV, 200 mA). Flash chromatography was performed on silica gel I-6-40 (YMC) of particle size 40-63 μm and on aluminum oxide 90 standardized (Merck 63-200 μm). Melting points were measured on a Yamato MP-21 and reported uncorrected. All commercially available compounds and solvents were used without further purification except for THF (distilled from Na by using benzophenone as an indicator) and CH_3CN (distilled from CaH_2 and P_4O_{10}).

Preparation of (*M*)-**2**-**2a**$^{2+}$(TfO^-)$_2$

Diacridine *rac*-**2**-**4a** was resolved by a recycle-type chiral HPLC (SUMICHIRAL OA-2000 column, 25 ˚C, hexane : CH_2Cl_2 = 1 : 1, 0.5% v/v Et_3N).[8] The first fraction [(*M*)-**2**-**4a**] was treated with CH_3OTf as in the case of *rac*-**2**-**4a** (**1**-**5b**). Optically active (*M*)-**2**-**2a**$^{2+}$(TfO^-)$_2$ salt was isolated in 13% yield.

CD (CH3CN): λ_{ext} / nm ($\Delta\varepsilon$ / M^{-1} cm^{-1}) 422 (+3.73), 390 (+0.818), 270 (-36.4), 258 (+33.0), 210 (-30.0).

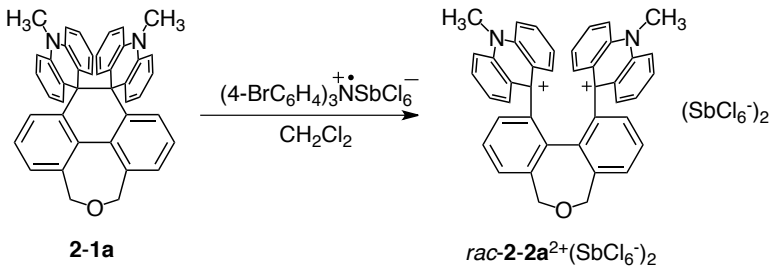

Preparation of 5,7-dihydrodibenz[*c*,*e*]oxepin-1,11-diylbis(10-methyl-9-acridinium) *rac*-**2-2a**$^{2+}$($SbCl_6^-$)$_2$

To a solution of **2-1a** (46.7 mg, 80.4 μmol) in dry CH_2Cl_2 5 mL was added tris(4-bromophenyl)ammoniumyl hexachloroantimonate (131 mg, 160.6 μmol) under Ar, and the mixture was stirred at 25 ˚C for 0.5 h. Another portion of **2-1a** (10.5 mg, 18.1 μmol) was added to this suspension, and the mixture was stirred at 25 ˚C for 3 h. After removal of the solvent under reduced pressure, the remaining solid was triturated with dry Et_2O. The precipitates were filtered and washed with dry Et_2O, and dried *in vacuo* to give **2-2a**$^{2+}$($SbCl_6^-$)$_2$ (101.4 mg) as a yellow powder in 82% yield.

Data for **2-2a**$^{2+}$($SbCl_6^-$)$_2$: m.p. 239-244 ˚C (decomp.); ^{1}H NMR in CD_3CN was identical to that of **1-2b**$^{2+}$(TfO^-)$_2$; IR (KBr) ν cm^{-1} 3104, 2969, 2926, 2864, 1608, 1577, 1545, 1457, 1372, 1276, 1123, 1061, 1038, 765, 743, 709, 604 cm^{-1}.

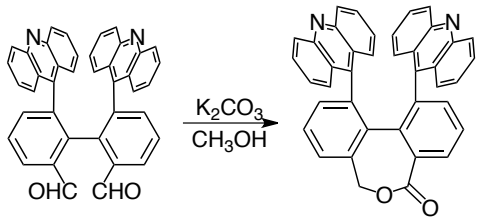

rac-**2-7** *rac*-**2-4b**

Preparation of 9,9'-(5,7-dihydro-4-oxo-dibenz[*c*,*e*]oxepin-1,11-diyl)diacridine *rac*-**2-4b**

A suspension of 9,9'-(6,6'-diformylbiphenyl-2,2'-diyl)diacridine **2-4b**[10] (150 mg, 266 μmol) and K_2CO_3 (220 mg, 1.59 mmol) in CH_3OH 6mL was stirred at 27 ˚C for 15.5 h. After diluted with water, the whole mixture was extracted with $CHCl_3$. The combined organic layers were washed with water and brine, and dried over anhydrous Na_2SO_4. After filtration, the crude reaction mixture was concentrated under reduced pressure. The residue was purified by recrystallization from EtOH to give **2-4b** (64.7 mg) as a yellow solid. Mother liquor was purified by flash chlomatography on silica gel ($CHCl_3$: EtOAc = 1 : 1 , 0.5% v/v Et_3N) to give **2-4b** (40.3 mg) as a yellow solid in a total yield of 70%.

Data for **2-4b**: m.p. > 300 ˚C; ^{1}H NMR (300 MHz, $CDCl_3$) δ 8.08 (1H, d, J = 8.8 Hz), 8.03 (1H, d, J = 8.8 Hz), 7.95 (1H, dd, J = 1.5 Hz, 7.9 Hz), 7.69 (1H, dd, J = 1.3 Hz, 7.9 Hz), 7.61 (2H, br-d, J = 7.9 Hz), 7.57 (1H, br-d, J = 6.0 Hz), 7.41 (2H, dd, J = 7.9 Hz, 7.9 Hz), 7.40 (1H, dd, J = 1.1 Hz, 7.9 Hz), 7.29-7.37 (3H, m), 7.23 (2H, d, J = 10.3 Hz), 7.14 (1H, ddd, J = 0.9 Hz, 6.4 Hz, 8.8 Hz), 7.03 (1H, dd, J = 1.5 Hz, 7.9 Hz), 6.98 (1H, dd, J = 1.3 Hz, 7.9 Hz), 6.70-6.77 (2H, m), 5.79 (1H, d, J = 8.8 Hz), 5.68 (1H, d, J = 8.4 Hz), 5.57 (1H, d, J = 11.7 Hz), 5.36 (1H, d, J = 11.7 Hz); IR (KBr) ν cm^{-1} 3063, 1728, 1626, 1608, 1554, 1538, 1517, 1460, 1436, 1407, 1370, 1353, 1263, 1227, 1083, 1013, 856, 818, 795, 751, 690, 649, 639, 629, 618, 612, 603 cm^{-1}; LR-MS (FD) m/z 564 (M^+, BP); Anal. Calcd. for $C_{40}H_{24}N_2O_2$•0.5EtOH: C 83.80, H 4.63, N 4.77. Found: C 83.84, H 4.40, N 4.65.

Optical resolution of *rac*-**2**-**4b**

Diacridine *rac*-**2**-**4b** was resolved by a recycle-type chiral HPLC (DAICEL CHIRALPAK IA column, 25 ˚C, hexane : CH_2Cl_2 = 1 : 1, 0.5% v/v EtOH).

The first fraction [(*M*)-**2**-**4b**]: CD (CH_2Cl_2): λ_{ext} / nm ($\Delta\varepsilon$ / M^{-1} cm^{-1}) 413 (-7.48), 376 (+30.9), 361 (+15.6), 332 (+0.03), 287 (+17.0), 278 (+11.0), 265 (+65.5), 257 (-5.92), 252 (+9.74), 238 (-45.5).

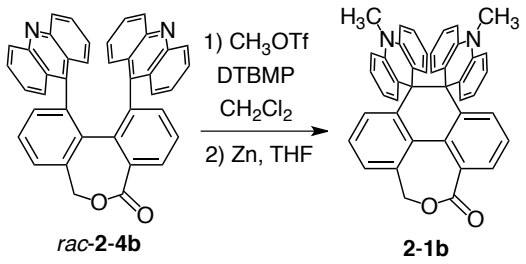

rac-**2-4b** **2-1b**

Preparation of dispiro[(10-methylacridan)-9,10'(4'H,6'H,10'H,11'H)-4-oxophenanthr[4',5'-*cde*]oxepin-11',9''-(10''-methylacridan)] **2-1b**

To a solution of *rac*-**2-4b** (64.8 mg, 114.7 μmol) and 2,6-di-tert-butyl-4-methylpyridine (46.5 mg, 227 μmol) in CH_2Cl_2 5 mL was added methyl trifluoromethanesulfonate (320 μL, 2.83 mmol) dropwise under Ar. After stirring for 18.5 h at 27 ˚C, the mixture was diluted and washed with dry Et_2O, and the solvent was evaporated To a suspension of the resulting salt in dry THF 5 mL was added Zn powder (300 mg, 4.59 mmol). The mixture was stirred for 28 h at 26 ˚C under Ar. After diluted with water, the whole mixture was extracted with CH_2Cl_2. The combined organic layers were washed with water and brine, and dried over anhydrous Na_2SO_4. After filtration, solvent was concentrated under reduced pressure. The residue was purified by flash chromatography on aluminum oxide (hexane : CH_2Cl_2 = 1 : 1, 0.5% v/v Et_3N) to give **2-1b** (33.2 mg) as a colorless powder in 49% yield over two steps.

Data for *rac*-**2-2b**$^{2+}$(TfO^-)$_2$: ^{1}H NMR in CD_3CN was identical to that of **2-2b**$^{2+}$ ($SbCl_6^-$)$_2$ described below; LR-MS (FAB) *m*/*z* = 594 (M^+, 11), 561 (25); HR-MS (FAB): Calcd. for $C_{42}H_{30}N_2O_2$: 594.2309, Found : 594.2277.

Data for **2-1b**: m.p. > 300 ˚C; ^{1}H NMR (300 MHz, $CDCl_3$) δ 7.90 (1H, dd, 1.8 Hz, 7.1 Hz), 7.44 (1H, dd, *J* =1.8 Hz, 6.6 Hz), 7.19-7.35 (4H, m), 6.99 (4H, ddd, *J* = 1.8 Hz, 8.3 Hz, 8.3 Hz), 6.79 (1 H, d, *J* = 7.9 Hz), 6.38-6.64 (7H, m), 6.20 (2H, br-s), 5.77 (1H, d, 7.3 Hz), 5.71 (1H, d, *J* = 7.2 Hz), 5.39 (1H, d, *J* = 12.5 Hz), 5.22 (1H, d, *J* = 12.5 Hz), 2.73 (3H, s), 2.72 (3H, s),; IR (KBr) ν cm^{-1} 3069, 2961, 2871, 2820, 1720, 1591, 1475, 1427,1383, 1363, 1324, 1280, 1245, 1169, 1135, 1101, 1059, 1039, 896, 863, 793, 750, 699, 657; LR-MS (EI) *m*/*z* 594 (M^+, BP), 579 ($[M\text{-}CH_3]^+$, 98), 535 ($[M\text{-}CH_3\text{-}CO_2]^+$, 9.7), 446 (11), 368 (12), 297 (M^{2+}, 21), 278 (74), 185 (13), 171 (11), 157 (16), 129 (29), 97 (24), 83 (28), 57 (51); Cyclic voltammetry (in CH_3CN, 0.1 M Et_4NClO_4, 0.1 V s^{-1}): E^{ox} = +0.27 V *vs.* SCE (irrev.); Anal. Calcd. for $C_{42}H_{30}N_2O_2$•0.5H_2O: C 83.56, H 5.18, N

4.64. Found: C 83.28, H 5.23, N 4.60

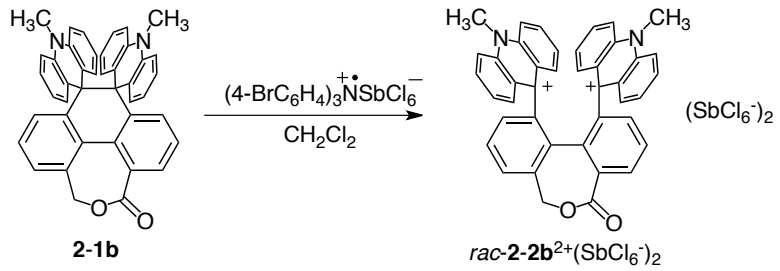

2-1b *rac*-**2-2b**$^{2+}$(SbCl$_6^-$)$_2$

Preparation of 4-oxo-5,7-dihydrodibenz[*c*,*e*]oxepin-1,11-diylbis(10-methyl-9-acridinium) **2-2b**$^{2+}$(SbCl$_6^-$)$_2$

To a solution of **2-1b** (23.3 mg, 39.2 μmol) in dry CH_2Cl_2 2 mL was added tris(4-bromophenyl)ammoniumyl hexachloroantimonate (63.6 mg, 160.6 μmol) under Ar, and the mixture was stirred at 25 ˚C for 65 min. Another portion of **2-1b** (1.6 mg, 2.7 μmol) was added to this suspension, and the mixture was stirred at 25 ˚C for 4 h. The remaining solid was triturated with dry Et_2O. The precipitates were filtered and washed with dry Et_2O, and dried in vacuo to give **2-2b**$^{2+}$(SbCl$_6^-$)$_2$ (45.1 mg) as a yellow powder in 85% yield.

Data for **2-2b**$^{2+}$(SbCl$_6^-$)$_2$: m.p. 239-244 ◦C (decomp.); ^{1}H NMR (300 Hz, CD_3CN) 8.46 (2H, dd, *J* = 7.9 Hz, 8.8 Hz), 8.29 (1H, dd, *J* = 1.5 Hz, 6.4 Hz, 9.3 Hz), 8.26 (1H, dd, *J* = 1.5 Hz, 6.8 Hz), 8.07-8.14 (1H, m), 8.08 (2H, dd, *J* = 1.5 Hz, 7.9 Hz), 8.02 (1H, br-d, *J* = 8.8 Hz), 8.00 (2H, dd, *J* = 1.1 Hz, 7.9 Hz), 7.63-7.72 (1H, m), 7.68 (2H, dd, *J* = 7.9 Hz, 7.9 Hz), 7.59 (2H, dd, *J* = 7.9 Hz, 7.9 Hz), 7.54 (1H, dd, *J* = 1.1 Hz, 8.6 Hz), 7.32 (1H, ddd, *J* = 1.1 Hz, 6.4 Hz, 8.8 Hz), 7.27 (1H, ddd, *J* = 1.1 Hz, 6.4 Hz, 8.6 Hz), 7.13 (1H, dd, *J* = 1.5 Hz, 7.9 Hz), 7.06 (1H, dd, *J* = 1.5 Hz, 7.9 Hz), 6.41 (1H, dd, *J* = 1.1 Hz, 8.6 Hz), 6.29 (1H, br-d, *J* = 8.8 Hz), 5.66 (1H, d, *J* = 12.6 Hz), 5.50 (1H, d, *J* = 12.6 Hz), 4.54 (3H, s), 4.52 (3H, s); IR (KBr) ν cm^{-1} 3083, 2957, 1727, 1608, 1578, 1548, 1460, 1445, 1370, 1278, 1192, 1099, 1026, 1015, 765, 707, 653, 602 cm^{-1}; Anal. Calcd. for $C_{42}H_{30}Cl_{12}N_2O_2Sb_2$•0.5$Et_2O$: C 40.63, H 2.71, N 2.15, Found: C 40.34 H 2.74, N 2.14.

X-ray analysis

Crystal data for **2-2a**$^{2+}$($SbCl_6^-$)$_2$

Crystals were obtained by recrystallizing from CH_3CN/Et_2O. MF $C_{44}H_{38}Cl_2O_5Sb_2$, FW 1315.72, red needle, 0.60 x 0.01 x 0.01 mm^3, triclinic *P*-1, a = 12.073(4), b = 15.599(6), c = 27.406(11) Å, α = 81.941(18), β = 80.772(18), γ = 79.240(18)˚, V = 4972(3) Å^3, ρ (Z = 4) = 1.757 g cm^{-3}. A total of 3091 unique data ($2\theta_{max}$ = 61.1 ˚) were measured at T = 153 K by a Rigaku/MSC Mercury CCD apparatus (Mo Kα radiation, λ = 0.71070 Å). Numerical absorption correction was applied (μ = 17.726 cm^{-1}). The structure was solved by the direct method (SIR2004) and refined by the full-matrix least-squares method on F^2 with anisotropic temperature factors for non-hydrogen atoms All the hydrogen atoms were located at the calculated positions and refined with riding. The final $R1$ and R_w values are 0.0581 ($I > 2.0\sigma I$) and 0.0630 ($I > 2.0\sigma I$) for 3091 reflections and 1211 parameters. Estimated standard deviations are 0.007-0.04 Å for bond lengths and 0.2-1.7 ˚ for bond angles, respectively.

References

[1] a) P. M. S. Monk, R. J. Mortimer, D. R. Rosseinsky, Electrochromism: Fundamentals and Applications, VCH, Weinheim, 1995; b) P. M. S. Monk, R. J. Mortimer, D. R. Rosseinsky, Electrochromism and Electrochromic Devices, Cambridge University Press, Cambridge, 2007

[2] T. Suzuki, J. Nishida, T. Tsuji, *Angew. Chem. Int. Ed. Engl.* **1997**, *36*, 1329.

[3] T. Suzuki, R. Yamamoto, H. Higuchi, E. Hirota, M. Ohkita, T. Tsuji, *J. Chem. Soc. Perkin Trans. 2* **2002**, 1937.

[4] J. Nishida, T. Suzuki, M. Ohkita, T. Tsuji, *Angew. Chem. Int. Ed.* **2001**, *40*, 3251.

[5] T. Suzuki, Y. Ishigaki, T. Iwai, H. Kawai, K. Fujiwara, H. Ikeda, Y. Kano, K. Mizuno, *Chem. Eur. J.* **2009**, *131*, 16896.

[6] a) J. Daub, J. Salbeck, I. Aurbach, *Angew. Chem.* **1988**, *100*, 278.; *Angew. Chem. Int. Ed. Engl.* **1988**, *27*, 291.; b) L. Zelikovich, J. Libman, A. Shanzer, *Nature* **1995**, *374*, 790.; c) C. Westermeier. H.-C. Gallmeier, M. Komma, J. Daub, *Chem. Commun.* **1999**, 2427.; d) G. Beer, C. Niederalt, S. Grimme, J. Daub, *Angew. Chem.* **2000**, *112,* 3385.; *Angew. Chem. Int. Ed.* **2000**, *39*, 3252; e) H. Higuchi, E. Ohta, H. Kawai, K. Fujiwara, T. Tsuji, T. Suzuki, *J. Org. Chem.* **2003**, *68*, 6605.; f) E. Gomar-Nadal, J. Veciana, C. Rovira, D. B. Amabilino, *Adv. Mater.* **2005**, *17*, 2095.

[7] T. Suzuki, A. Migita, H. Higuchi, H. Kawai, K. Fujiwara, T. Tsuji, *Tetrahedron Lett.* **2003**, *44*, 6837.

[8] T. Nehira, Y. Yoshimoto, K. Wada, H. Kawai, K. Fujiwara, T. Suzuki, *Chem. Lett.* **2010**, *39*, 165.

[9] a) H. Hanawa, D. Uraguchi, S. Konishi, T. Hashimoto, K. Maruoka, *Chem. Eur. J.* **2003**, *9*, 4405; b) L. A. Arnold, R. Imbos, A. Mandoli, A. H. M. de Vries, R. Naasz, B. L. Feringa, *Tetrahedron* **2000**, 56, 2865; c) H.-Z. Tang, P. D. Boyle, B. M. Novak, *J. Am. Chem. Soc.* **2005**, *127*, 2136.

[10] T. Suzuki, Y. Yoshimoto, T. Takeda, H. Kawai, K. Fujiwara, *Chem. Eur. J.* **2009**, *15*, 2210.

Chapter 3
Construction of 9,9,10,10-tetraaryldihydrophenanthrene-type Dynamic Redox Systems working on Au surface

3-1 Introduction

Recently, many research about the surface immobilization of functional molecules such as sensors and molecular-based data storage device are reported[1]. One of the most important purpose of these research is the development of data storage device. Electrochemical bistability plays important roles for this purpose. Yet, successful construction of electrochemically bistable surface have rarely been reported[1e].

In the author's laboratory, electrochemically bistable redox systems are constructed by adopting the concept of dynamic redox systems[2], whose C-C bond is cleaved/formed upon redox reactions. In these systems, two different molecular structures of redox species change their reduction and oxidation potential.

By fixing the dynamic redox systems on a solid surface, construction of electrochemically bistable functional surface, which can work as a high-density memory device, could be realized. According to this scenario, diolefin-type dynamic redox system **3-I**/**3-II**$^{2+}$ with anchoring group were investigated by E. Ohta[3]. This molecule was immobilized on Au electrode by the lipoic ester, and previously its redox reaction was conducted on Au surface (Scheme 3-1). Yet, this system has some problems such as instability of redox species, and existence of long-lifetime intermediate of redox reactions, which should be inconvenience for further pursuing the unimolecular switching function.

Scheme 3-1

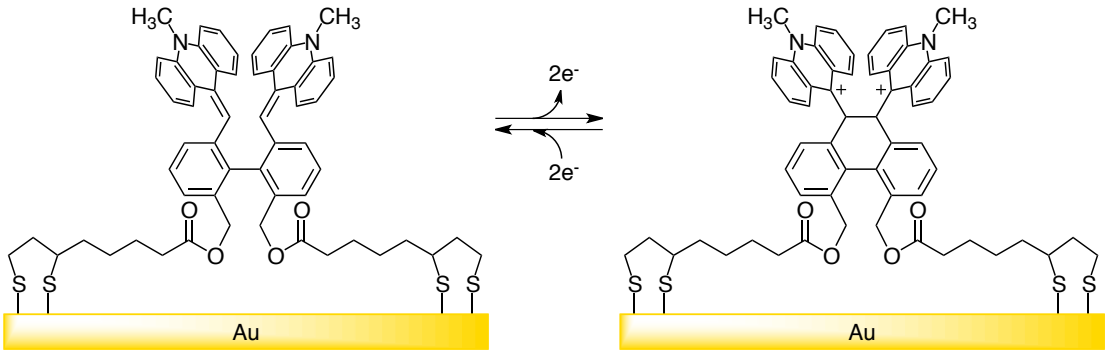

3-I/Au **3-II**$^{2+}$/Au

In this chapter, the author newly designed the tetraaryldihydrophenanthrene-based redox systems with anchoring groups. By considering the stability of both neutral and dicationic states, the 10-methylacridan/acridinium skeletons were again used as redox-active moieties. Lipoic ester moiety was selected as anchoring groups for its stable disulfide bond. In addition, in order to avoid the influence of stereoisomerism by an asymmetric center in the five-membered ring of lipoic ester, higher symmetric isomer of lipoic ester (isolipoic ester[4]) was also investigated (Scheme 3-2).

Scheme 3-2

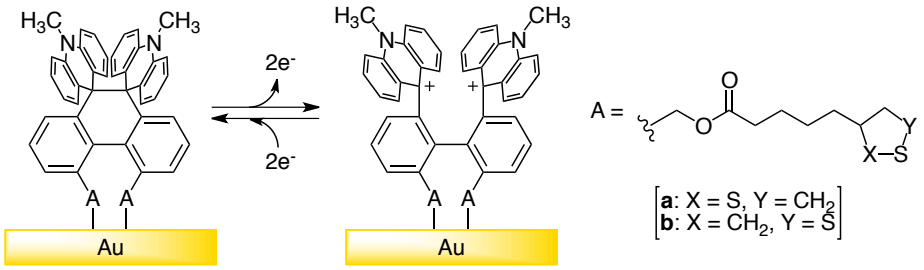

3-1/Au **3-2**$^{2+}$/Au

3-2 Preparation

Preparation was carried out similar to the case of acetate (Chapter 1). Thus diol **3-3** was condensed with *DL*-α-lipoic acid or isolipoic acid by 1-ethyl-(3-dimethylaminopropyl)carbodiimide (EDCI) and 4-dimethylaminopyridine (DMAP) to give donors **3-1a**,**b** in 59 and 71% yield, respectively. To confirm that tetraaryldihydrophenanthrene moiety can be oxidized without damaging lipoic ester part, donor **3-1a** was subjected to chemical oxidation by two equivalents of $(4\text{-}BrC_6H_4)_3N^{+\bullet}SbCl_6^-$, which gave the corresponding dication salt **3-2a**$^{2+}(SbCl_6^-)_2$ in 44% yield (Scheme 3-3).

Scheme 3-3

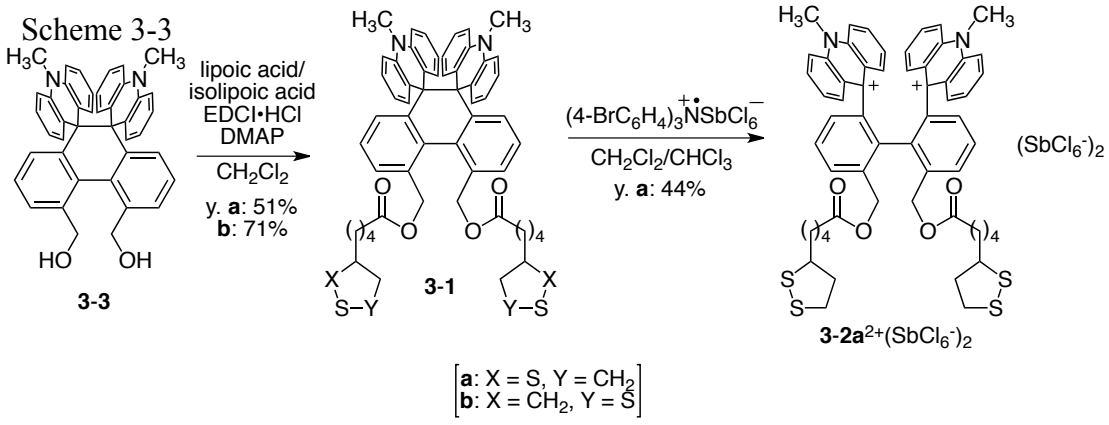

3-3 Redox properties of 3-1/3-2^{2+}

3-3-1 Voltammetric analyses in solution state

First, redox properties of donors **3-1a**,**b** were investigated in CH_2Cl_2, whose results give information on the solution-state properties. As shown in Figure 3-1, oxidation and reduction peaks are observed separately (**a**: E^{ox} = + 0.56 V *vs.* Ag/AgCl, E^{red} = - 0.10 V *vs.* Ag/AgCl; **b**: E^{ox} = -0.69 V *vs.* Ag/AgCl, E^{red} = -0.23 V *vs.* Ag/AgCl). These separated redox peaks are characteristic to the dynamic redox systems[3],[5], showing that introduction of lipoic ester moiety does not affect the dynamic redox behavior. of the tetrraryldihydrophenanthrene moiety.

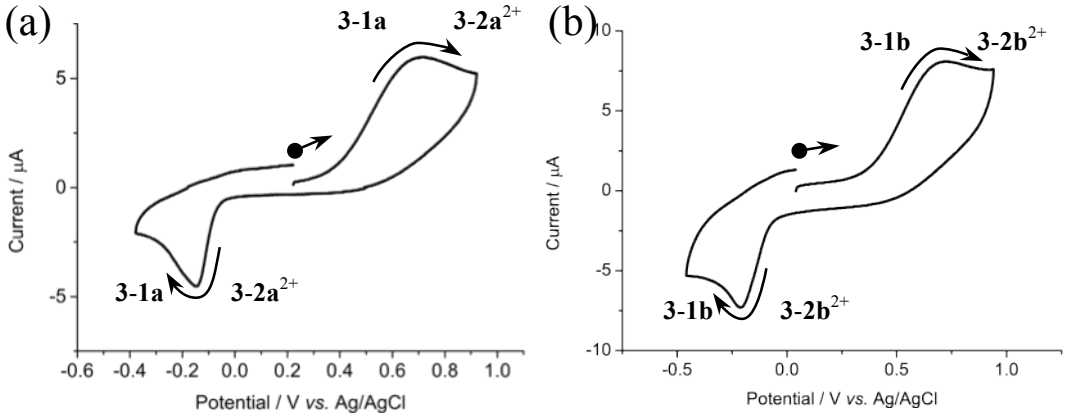

Figure 3-1. Cyclic voltammograms of (a) **3-1a** and (b) **3-1b** in 0.1 M Bu_4NClO_4 solution at scan rate of 500 mV s^{-1}. Pt working and counter electrodes were used.

3-3-2 Voltammetric analyses on Au(111) electrode

After confirmation of dynamic redox behavior has finished in solution state, voltammetric analyses in were conducted. Surface immobilization on Au(111) electrode was carried out by immersing a freshly prepared Au(111) electrode into a CH_2Cl_2 solution containing **3-1a**,**b** (100 μM) for 1 h and 30 min., respectively. The surface coverage was estimated to be 5 x 10^{13} molecules cm^{-2} by integrating the current of a 2e-reduction wave (*vide supra*), These values are reasonable compared to the value of non-subsituted alkanethiol (10^{14} molecules cm^{-2})[6] and considering the bulkiness of headgroup.

In the voltammograms of immobilized donor (**3-1a**,**b**/Au), the separation of redox peaks are much narrower (**a**: E^{ox} = -0.19 V *vs.* Ag/AgCl, E^{red} = -0.38 V *vs.* Ag/AgCl; **b**:

E^{ox} = -0.18 V *vs.* Ag/AgCl, E^{red} = -0.30 V *vs.* Ag/AgCl) (Figure 3-2) than that measured in CH_2Cl_2. This narrow peak separation may suggest that the electrochemical bistability is smaller on gold surface. Similar redox behavior was observed in isolipoic ester **3-1b**.

Thus, spectroscopic investigation are carried out to confirm that the redox species on Au surface are identical to those in solution.

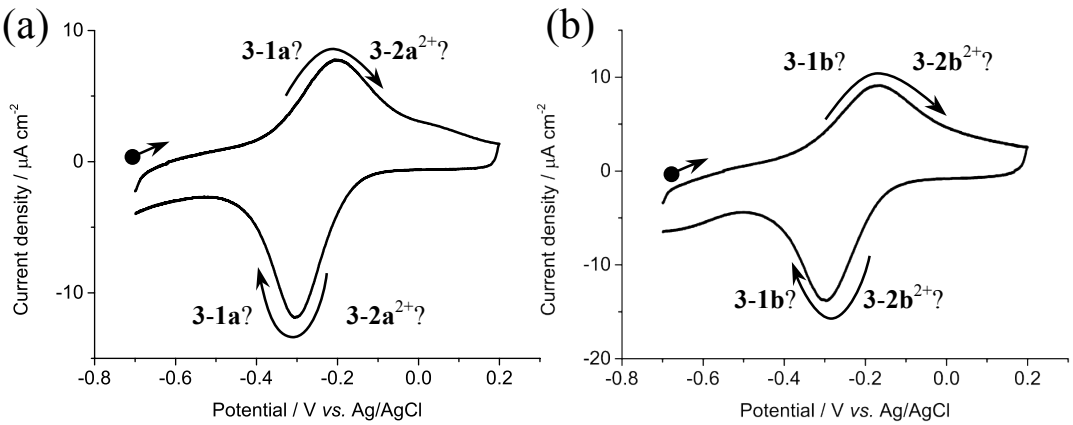

3-4 Characterization of redox species on Au by IR spectroscopic investigation

In order to identify the redox species, IR spectral changes upon potential steps were observed by the Surface-Enhanced Infrared Absorption Spectroscopy (SEIRAS) method. Donor **3-1a** was immobilized on gold thin film constructed on a Si prism as in the case of Au(111) electrode, and then the sample was put in a electrochemical cell. The potential was stepped from a cathodic region (-0.7 V *vs.* Ag/AgCl) to an anodic region (+0.2 V *vs.* Ag/AgCl). Observed spectral changes were as shown in Figure 3-3. By comparing with the spectra of isolated **3-1a**/**3-2a**$^{2+}$($SbCl_6^-$)$_2$ in KBr tablet dice, it

Figure 3-2. Cyclic voltammograms of (a) **3-1a**/Au and (b) **3-1b**/Au in 0.1 M $NaClO_4$ aqueous solution at scan rate of 100 mV s^{-1}. Pt counter electrodes were used.

was found that decrease in signals of donor **3-1a** and increase in signals of dication **3-2a**$^{2+}$, thus oxidation of donor **3-1a** to dication **3-2a**$^{2+}$, occur upon positive potential steps. Similarly, reduction of **3-2a**$^{2+}$ to donor **3-1a** was observed upon negative potential steps. This electrochemical response indicates that the redox peaks observed on gold electrode comes from the redox reactions between **3-1a** and **3-2a**$^{2+}$.

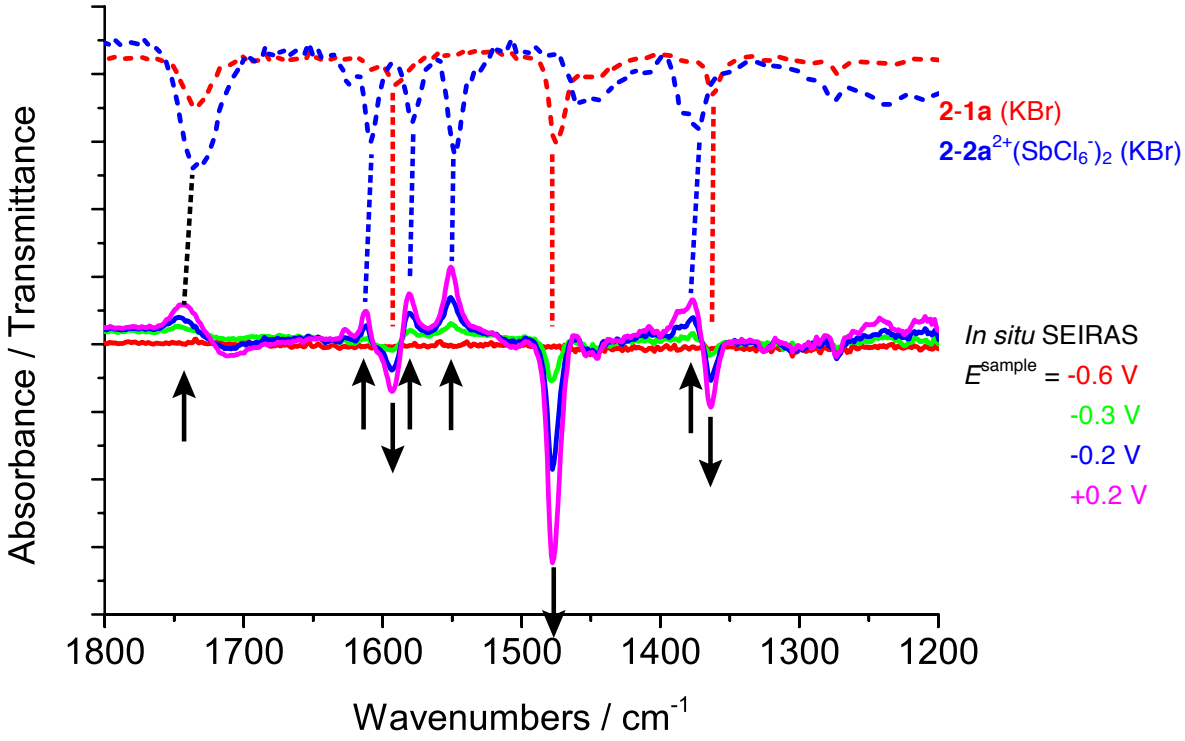

Figure 3-3. IR spectra of **3-1a** and **3-2a**$^{2+}$$(SbCl_6^-)_2$ in KBr tablet dice (upper) and *in situ* IR spectra of **3-1a**/Au (lower) obtained by ATR method upon potential steps from -0.7 V to +0.2 V *vs.* Ag/AgCl. (E^{ref} = +0.7 V)

3-5 Summary

In this work, the author desiginend and constructed the novel hexaphenylethane-type redox systems with lipoic and isolipoic esters. Redox pair **3-1**/**3-2**$^{2+}$ can be immobilized on Au(111) electrode, and their redox reactions were conducted on Au surface. Their electrochemical bistability was found to differ in CH_2Cl_2 solution and fixed on Au(111) surface. Such difference of redox behavior have not been found in these dynamic redox systems, thus this result can provide another interest in C-C bond formation/cleavage upon redox reactions. Lipoic ester and isolipoic ester showed no significant differences in redox properties, showing stereoisomer does not so affect the redox properties[4] so much.

Experimental section

General

^{1}H and ^{13}C NMR spectra were recorded on a JEOL AL-300 (^{1}H 300 MHz and ^{13}C 75 MHz) and Bruker Ascend 400 spectrometer (^{1}H 400 MHz). Chemical shifts (δ) were reported with TMS (in $CDCl_3$, δ=0.00 ppm) or CH_3CN (in CD_3CN, δ=1.93 ppm) as internal standards. IR spectra in KBr tablet dice were recorded on a JEOL WINSPEC100 infrared spectrophotometer. *In situ* IR spectra were recorded on a Bio-Rad FTS-60A/896 infrared spectrometer with Tohogiken Polarization unit PS-06. Mass spectra were recorded on a JEOL JMS-600H in EI mode, and on a JMS-AX500 spectrometers in FD mode (GC-MS & NMR Laboratory, Graduate School of Agriculture, Hokkaido University). Elemental Analyses were taken on J-Science micro corder JM10 or on a Yanaco CHN corder MT-6 at the Instrumental Analysis Division, Equipment Management Center, Creative Research Institution, Hokkaido University. Cyclic voltammograms in CH_2Cl_2 were measured with a BAS ALS-600A electrochemical analyzer. Cyclic voltammograms on Au were measured with this apparatus or a Hokuto Denko HSV-100 automatic polarization system. X-ray diffraction data for single-crystal analysis were measured by a RIGAKU AFC-5R + Mercury CCD apparatus (50 kV, 200 mA). Flash chromatography was performed on silica gel I-6-40 (YMC) of particle size 40-63 μm and on aluminum oxide 90 standardized (Merck 63-200 μm). Melting points were measured on a Yamato MP-21 and reported uncorrected. UV-Vis spectra were recorded on a Hitachi U-3500 spectrophotometer. Fluorescence spectra were measured on a Hitachi F-4500 spectrofluorometer. All commercially available compounds and solvents were used without further purification except for THF (distilled from Na by using benzophenone as an indicator, or purified by Nikko Hansen GlassContour Solvent Dispensing System) and CH_3CN (distilled from CaH_2 and P_4O_{10}).

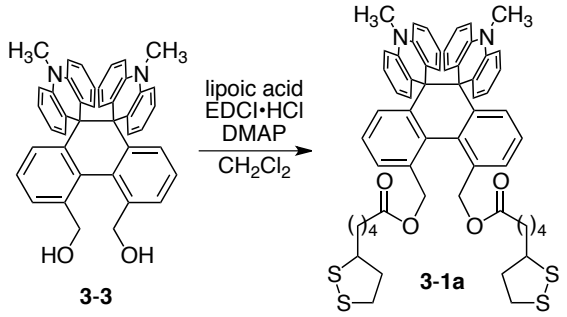

3-3 **3-1a**

Preparation of lipoic ester **3-1a**

To a solution of **3-3** (51.8 mg, 86.5 μmol) and DMAP (one crystal) in dry CH_2Cl_2 5 mL was added *DL*-α-lipoic acid (54.0 mg, 262 μmol) and 1-ethyl-3-(3-dimethylaminopropyl)carbodiimide hydrochloride (EDCI•HCl, 50.1 mg, 261 μmol) at 25 ˚C, and the mixture was stirred for 16 h at this temperature. After addition of water, the resultant mixture was extracted with CH_2Cl_2, then the organic layer was washed with brine and dried over Na_2SO_4. Chromtatographic purification (Al_2O_3, hexane:EtOAc = 4:1, 0.5% v/v triethylamine (Et_3N)) gave **3-1a** as a pale yellow powder (50.0 mg) in 59% yield.

Data for **3-1a**: m.p.: 97˚C-101˚C (decomp. for mixtures of diastereomers); ^{1}H NMR (300 MHz, $CDCl_3$) δ 7.42 (2H, d, J = 6.3 Hz), 7.19 (2H, dd, J = 6.3 Hz, J = 6.3 Hz,), 7.08 (2H, d, J = 6.3 Hz), 6.98 (4H, br-dd, J = 8.3 Hz, 8.3 Hz), 6.89 (2H, d, J = 8.3 Hz), 6.56 (2H, d, J = 8.3 Hz), 6.48 (2H, dd, J = 8.3 Hz, 8.3 Hz), 6.42 (2H, d, J = 8.3 Hz), 6.20 (2H, dd, J = 8.3 Hz, 8.3 Hz), 5.65 (2H, d, J = 8.3 Hz), 5.43 (2H, d, J = 12.6 Hz). 5.34 (2H, d, J = 12.6 Hz), 3.52-3.57 (2H, qn, J = 6.4 Hz), 3.07-3.17 (4H, m), 2.70 (6H, s), 2.33-2.50 (6H, m), 1.83-1.96 (2H, m), 1.62-1.76 (8H, m), 1.43-1.54 (4H, m); ^{13}C NMR (75 MHz, $CDCl_3$) δ 173.20, 144.25, 144.16, 142.75, 135.09, 132.51, 132.44, 131.98, 131.88, 128.15, 127.66, 127.36, 127.29, 125.17, 124.65, 119.07, 116.80, 112. 07, 110.21, 64.49, 58.72, 56.28, 40.19, 38.49, 34.61, 34.09, 33.87, 28.76, 24.68; IR (KBr) ν cm^{-1}; 3058, 2926, 1735, 1590, 1474, 1361, 1269, 1166, 754; FD-LR-MS m/z 974 (M^+, BP), 487 (M^{2+}, 3.7); Anal. Calcd. for $C_{58}H_{58}N_2O_4S_4$: C, 71.42; H, 5.99; N, 2.87. Found: C, 71.15; H, 5.91; N, 2.92.

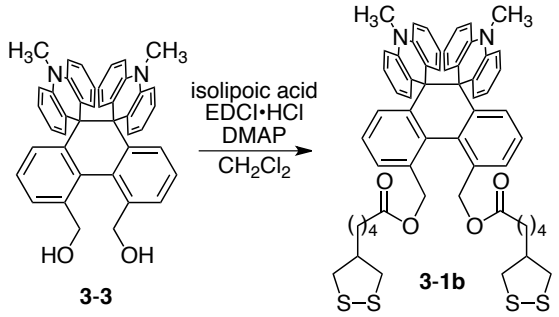

Preparation of isolipoic ester **3-1b**

To a solution of **3-3** (111 mg, 186 μmol) and DMAP (2.4 mg, 19.6 μmol) in dry CH_2Cl_2 5 mL was added isolipoic acid (116 mg, 561 μmol) and EDCI•HCl (48.2 mg, 593 μmol) at 23 ˚C, and the mixture was stirred for 6.5 h at this temperature. After addition of water, the resultant mixture was extracted with CH_2Cl_2, then the organic layer was washed with brine and dried over Na_2SO_4. Chromtatographic purification (Al_2O_3, hexane:EtOAc = 4:1 0.5% v/v triethylamine (Et_3N)) gave **3-1b** as a pale yellow powder (122 mg) in 67% yield.

Data for **3-1b**: m.p.: 103˚C-106˚C ; ^{1}H NMR (300 MHz, $CDCl_3$) δ 7.57 (2H, d, J = 7.8 Hz), 7.19 (2H, dd, J = 6.8 Hz, 6.8 Hz), 7.08 (2H, d, J = 6.8 Hz), 6.98 (4H, br-dd, J = 8.6 Hz, 8.6 Hz), 6.89 (2H, d, J = 8.6 Hz), 6.56 (2H, d, J = 8.6 Hz), 6.48 (2H, dd, J = 8.6 Hz, 8.6 Hz), 6.43 (2H, d, J = 8.6 Hz), 6.18 (2H, dd, J = 8.6 Hz, 8.6 Hz), 5.65 (2H, d, J = 8.6 Hz), 5.43 (2H, d, J = 12.3 Hz), 5.34 (2H, d, J = 12.3 Hz), 3.21 (4H, m), 2.76 (4H, dd, J = 6.8 Hz, 11.0 Hz), 2.70 (6H, s), 2.51 (2H, qn, J = 6.8 Hz), 2.37 (4H, td, J = 6.8 Hz, 7.5 Hz), 1.67 (4H, qn, J = 7.5 Hz), 1.47-1.54 (4H, m), 1.36-1.45 (4H, m); ^{13}C NMR (75 MHz, $CDCl_3$) δ 173.07, 144.15, 144.03, 142.67, 135.01, 132.34, 132.34, 131.85, 131.75, 128.02, 127.54, 127.29, 127.18, 125.04, 124.45, 118.91, 116.74, 112.02, 110.16, 64.37, 58.60, 47.47, 43.85, 33.97, 33.81, 33.36, 27.96, 24.80; IR (KBr) ν cm^{-1};3058, 3038, 2925, 2867, 1732, 1607, 1590, 1474, 1444, 1362, 1271, 1166, 1133, 1057, 754, 733, 698; FD-MS m/z 974 (M^+, BP), 487.2 (M^{2+}, 11); Anal. Calcd. for $C_{58}H_{58}N_2O_4S_4$: C, 71.42; H, 5.99; N, 2.87. Found: C, 71.24; H, 6.06; N, 2.67.

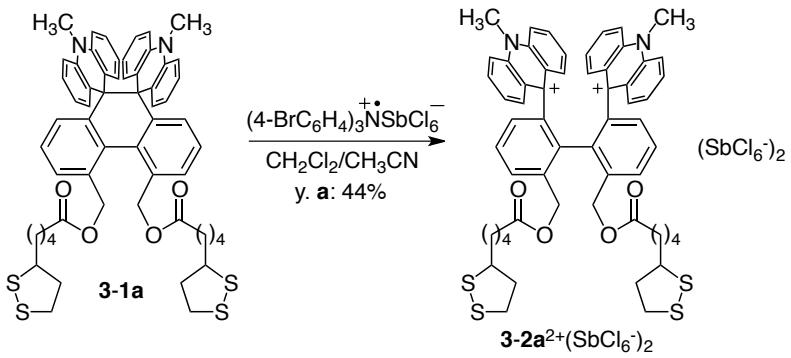

Oxidation of donor **3-1a** to dication salt **3-2a**$^{2+}$($SbCl_6^-$)$_2$

To a solution of **3-1a** (46.6 mg, 47.8 μmol) in dry CH_2Cl_2 5 mL was added a solution of tris(4-bromophenyl)ammoniumyl hexachloroantimonate (77.4 mg, 94.8 μmol) in dry CH_3CN 10 mL at 26 ˚C, and the mixture was stirred for 30 min at this temperature. After removal of the solvent under reduced pressure, the remaining solid was triturated with dry Et_2O. The precipitates were filtered and washed with dry Et_2O, and dried *in vacuo* to give **2-2a**$^{2+}$($SbCl_6^-$)$_2$ (34.6 mg) as a brown powder in 44% yield.

Data for **3-2a**$^{2+}$($SbCl_6^-$)$_2$: m.p.: 148 ˚C-152 ˚C (decomp.); ^{1}H NMR (400 MHz, CD_3CN) δ 8.49 (2H, d, J = 8.4 Hz), 8.37 (2H, dd, J = 8.0 Hz, 8.0 Hz), 8.10 (2H, br-dd, J = 7.0 Hz, 7.0 Hz), 8.03 (2H, d, J = 8.4 Hz), 7.91 (2H, d, J = 7.0 Hz), 7.84 (2H, d, J = 8.0 Hz), 7.83 (2H, dd, J = 8.4 Hz, 8.4 Hz), 7.60 (2H, dd, J = 8.4 Hz, 8.4 Hz), 7.18 (2H, dd, J = 8.0 Hz, 8.0 Hz), 6.96 (2H, d, J = 7.0 Hz), 6.13 (2H, d, J = 8.4 Hz), 5.43 (2H, d, J = 13.2 Hz), 5.29 (2H, d, J = 13.2 Hz), 4.56 (6H, s) 3.69 (2H, qn, J = 8.0 Hz), 3.13-3.27 (4H, m), 2.64 (4H, t, J = 8.0 Hz), 2.51 (2H, sx, J = 6.0 Hz), 1.56-1.90 (14H, m); IR (KBr) ν cm^{-1}; 3087, 2928, 2855, 1732, 1608, 1578, 1548, 1460, 1373, 1168, 765; FD-LR-MS m/z 974 (M^+, BP), 959 ([M-CH_3]$^+$, 22), 944 ([M-2CH_3]+, 67), 487 (M^{2+}, 10); FD-HR-MS Calcd. for $C_{58}H_{58}N_2O_4S_4$: 974.3279; Found: 974.3294.

References

[1] a) S. R. Bayly, T. M. Gray, M. J. Chmielewski, J. J. Davis, P. D. Beer, *Chem. Commun.* **2007**, 2234.; b) W. R. Browne, B. L. Feringa, Annu. Rev. Phys. Chem. 2009, 60, 407.; c) R. A. van Delden, K. J. ter Wiel, M. M. Pollard, J. Vicario, N. Koumura, B. L. Feringa, *Nature* **2005**, *437*, 1337.; d) N. Katsonis, M. Lubomska, M. M. Pollard, B. L. Feringa, P. Rudolf, *Prog. Surf. Sci*. **2007**, *82*, 407.; e) O. Ivashenko, H. Logtenberg, J. Areephong, A. C. Coleman, P. V. Wesenhagen, E. M. Geertsema, N. Heureux, B. L. Feringa, P. Rudolf, W. R. Browne, *J. Phys. Chem. C.* **2011**, *115*, 22965.;

[2] T. Suzuki, E. Ohta, H. Kawai, K. Fujiwara, T. Fukushima, *Synlett* **2007**, 851.

[3] E. Ohta, Ph. D. Thesis, Hokkaido University (2008)

[4] K. M. Joly, G. Mirri, Y. Willenere, S. L. Horswell, C. J. Moody, and J. H. R. Tucker, *J. Org. Chem.* **2010**, *75*, 2395.

[5] T. Suzuki, A. Migita, H. Higuchi, H. Kawai, K. Fujiwara, T. Tsuji, *Tetrahedron Lett.* **2003**, *44*, 6837.

[6] a) M. M. Alkaisi;R. J. Blaikie, S. J. McNab, *Adv. Mater.* **2001**, *13*, 877.; b) A. Lewis, *Phys. World* **2001**, *14*, 25. c) J. Jiang, K. Bosnick, M. Maillard, L. Brus, *J. Phys. Chem. B* **2003**, *107*, 9964.; d) M. J. Levene, J. Korlach, S. W. Turner, M. Foquet, H. G. Craighead, W. W. Webb, *Science* **2003**, *299*, 682. e) L. H. Dubois, L. H., R. G. Nuzzo, *Annu. Rev. Phys. Chem.* **1992**, *43*, 437.

Acknowledgement

This work has been carried out under the direction of Professor Dr. Takanori Suzuki, Department of Chemistry, Faculty of Science, Hokkaido University. The author would love to express his sincere gratitude to Professor Suzuki for his consistent guidance, suggestion, valuable discussions, encouragement, and so much help throughout the course of this work.

The author deeply grateful to Professor Dr. Kenshu Fujiwara, Professor Dr. Hidetoshi Kawai, Professor Dr. Ryo Katoono, for their kind guidance, suggestion, valuable discussions, encouragement, and so much help of this work.

The author would like to express his deep gratitude to Professor Dr. Kohei Uosaki, Professor Dr. Hidenori Noguchi, Professor Dr. Takuya Masuda, Dr. Mikio Ito, and Dr. Yukihisa Okawa, International Center for Materials Nanoarchitectonics (MANA)/ Global Research Center for Environment and Energy based on Nanomaterials Science, National Institute for Materials Science, for the electrochemical investigation, valuuable discussions, and directions in Chapter 3. The author is thanking for giving opportunities to study in Professor Uosaki's laboratory and expresses his appreciation to all members of Professor Uosaki's group.

The author is indebted to Professor Dr. Masaya Sawamura, Professor Dr. Masako Kato, Department of Chemistry, Faculty of Science, Hokkaido University, and Professor Dr. Hajime Ito, Division of Chemical Process Engineering and Frontier Chemistry Center, Graduate School of Engineering, Hokkaido University for their participation to the preliminary examination of this dissertation and helpful discussions.

The author is really thankful to Dr. Eri Fukushi, Mr. Kenji Watanabe and Mr. Yusuke Takata, GC-MS & NMR Laboratory, Graduate School of Agriculture, Hokkaido University, for the measurement of mass spectra. The author is deeply grateful to Ms. Miwa Kiuchi, Ms. Tomo Hattori, Ms. Nao Saito, and Ms. Yukako Sasaki, Instrumental Analysis Division, Equipment Management Center, Creative Research Institution, Hokkaido Univeristy, for the measurement of elemental analyses.

The author gives a special thanks to Dr. Eisuke Ohta, Dr. Takashi Takeda, Dr. Hiroyoshi Sugino, Ms. Yasuyo Yoshimoto, Dr. Yusuke Ishigaki, Dr. Youhei Miura, Mr. Yoshinori Tani, Dr. Keita Tanaka, Ms. Fumi Oba, Ms. Yuki Ono, Mr. Yuuki Hoshiyama, and other members of Professor Suzuki's group for their valuable discussions and giving him invaluable time.

Finally, the author would like to express his deep and sincere graditude to his family for their continuous help and encouragement.

Kazuhisa Wada